the axenic cultivation of *Entamoeba histolytica* and other *Entamoeba*. Trans. R. Soc. Trop. Med. Hyg. **72**:431–432.

10. **Gillin, F. D., P. Hagblom, J. Harwood, S. B. Aley, D. S. Reiner, M. McCaffery, M. So, and D. G. Guiney.** 1990. Isolation and expression of the gene for a major surface protein of *Giardia lamblia*. Proc. Natl. Acad. Sci. USA **87**:4463–4467.
11. **Haque, R., C. D. Huston, M. Hughes, E. Houpt, and W. A. Petri, Jr.** 2003. Amebiasis. N. Engl. J. Med. **348**:1565–1573.
12. **Kimura, A., Y. Hara, T. Kimoto, Y. Okuno, Y. Minekawa, and T. Nakabayashi.** 1996. Cloning and expression of a putative alcohol dehydrogenase gene of *Entamoeba histolytica* and its application to immunological examination. Clin. Diagn. Lab. Immunol. **3**:270–274.
13. **Laemmli, U. K.** 1970. Cleavage of structural proteins during the assembly of the head of bacteriophage T4. Nature **227**:680–685.
14. **Lotter, H., E. Mannweiler, M. Schreiber, and E. Tannich.** 1992. Sensitive and specific serodiagnosis of invasive amebiasis by using a recombinant surface protein of pathogenic *Entamoeba histolytica*. J. Clin. Microbiol. **30**: 3163–3167.
15. **Petri, W. A., Jr., M. D. Chapman, T. Snodgrass, B. J. Mann, J. Broman, and J. I. Ravdin.** 1989. Subunit structure of the galactose and *N*-acetyl-D-galactosamine-inhibitable adherence lectin of *Entamoeba histolytica*. J. Biol. Chem. **264**:3007–3012.
16. **Petri, W. A., Jr., R. Haque, and B. J. Mann.** 2002. The bittersweet interface of parasite and host: lectin-carbohydrate interactions during human invasion by the parasite *Entamoeba histolytica*. Annu. Rev. Microbiol. **56**:39–64.
17. **Rivera, W. L., H. Tachibana, M. R. Silva-Tahat, H. Uemura, and H. Kanbara.** 1996. Differentiation of *Entamoeba histolytica* and *E. dispar* DNA from cysts present in stool specimens by polymerase chain reaction: its field application in the Philippines. Parasitol. Res. **82**:585–589.
18. **Shenai, B. R., B. L. Komalam, A. S. Arvind, P. R. Krishnaswamy, and P. V. Rao.** 1996. Recombinant antigen-based avidin-biotin microtiter enzyme-linked immunosorbent assay for serodiagnosis of invasive amebiasis. J. Clin. Microbiol. **34**:828–833.
19. **Soong, C. J., K. C. Kain, M. Abd-Alla, T. F. Jackson, and J. I. Ravdin.** 1995. A recombinant cysteine-rich section of the *Entamoeba histolytica* galactose-inhibitable lectin is efficacious as a subunit vaccine in the gerbil model of amebic liver abscess. J. Infect. Dis. **171**:645–651.
20. **Soong, C. J., B. E. Torian, M. D. Abd-Alla, T. F. Jackson, V. Gatharim, and J. I. Ravdin.** 1995. Protection of gerbils from amebic liver abscess by immunization with recombinant *Entamoeba histolytica* 29-kilodalton antigen. Infect. Immun. **63**:472–477.
21. **Stanley, S. L., Jr.** 2003. Amoebiasis. Lancet **361**:1025–1034.
22. **Stanley, S. L., Jr., T. F. Jackson, S. L. Reed, J. Calderon, C. Kunz-Jenkins, V. Gathiram, and E. Li.** 1991. Serodiagnosis of invasive amebiasis using a recombinant *Entamoeba histolytica* protein. JAMA **266**:1984–1986.
23. **Tachibana, H., S. Kobayashi, X. J. Cheng, and E. Hiwatashi.** 1997. Differentiation of *Entamoeba histolytica* from *E. dispar* facilitated by monoclonal antibodies against a 150-kDa surface antigen. Parasitol. Res. **83**:435–439.
24. **Tachibana, H., S. Kobayashi, K. Nagakura, Y. Kaneda, and T. Takeuchi.** 2000. Asymptomatic cyst passers of *Entamoeba histolytica* but not *Entamoeba dispar* in institutions for the mentally retarded in Japan. Parasitol. Int. **49**: 31–35.
25. **Tachibana, H., S. Kobayashi, M. Takekoshi, and S. Ihara.** 1991. Distinguishing pathogenic isolates of *Entamoeba histolytica* by polymerase chain reaction. J. Infect. Dis. **164**:825–826.
26. **Towbin, H., T. Staehelin, and J. Gordon.** 1979. Electrophoretic transfer of proteins from polyacrylamide gels to nitrocellulose sheets: procedure and some applications. Proc. Natl. Acad. Sci. USA **76**:4350–4354.
27. **Walsh, J. A.** 1986. Problems in recognition and diagnosis of amebiasis: estimation of the global magnitude of morbidity and mortality. Rev. Infect. Dis. **8**:228–238.
28. **Zhang, Y., E. Li, T. F. Jackson, T. Zhang, V. Gathiram, and S. L. Stanley, Jr.** 1992. Use of a recombinant 170-kilodalton surface antigen of *Entamoeba histolytica* for serodiagnosis of amebiasis and identification of immunodominant domains of the native molecule. J. Clin. Microbiol. **30**:2788–2792.

Available online at www.sciencedirect.com
SCIENCE DIRECT
ELSEVIER
Molecular & Biochemical Parasitology 138 (2004) 195–203
MOLECULAR & BIOCHEMICAL PARASITOLOGY

Molecular characterization of peroxiredoxin from *Entamoeba moshkovskii* and a comparison with *Entamoeba histolytica*☆

Xun-Jia Cheng[a,b], Eisaku Yoshihara[c], Tsutomu Takeuchi[d], Hiroshi Tachibana[a,*]

[a] *Department of Infectious Diseases, Tokai University School of Medicine, Isehara, Kanagawa 259-1193, Japan*
[b] *Department of Medical Microbiology and Parasitology, Fudan University School of Medicine, Shanghai 200032, China*
[c] *Department of Molecular Life Sciences, Tokai University School of Medicine, Isehara, Kanagawa 259-1193, Japan*
[d] *Department of Tropical Medicine and Parasitology, Keio University School of Medicine, Shinjuku-ku, Tokyo 160-8582, Japan*

Received 12 August 2004; accepted 27 August 2004
Available online 2 October 2004

Abstract

Peroxiredoxin of the pathogenic parasite, *Entamoeba histolytica*, is thought to be involved in protection from oxidative attack by host phagocytic cells and endogenously generated hydrogen peroxide. In this study, we cloned peroxiredoxin genes from the nonpathogenic ameba, *Entamoeba moshkovskii*, and characterized the peroxiredoxin protein. The open reading frame of three cloned cDNAs was demonstrated to encode a polypeptide of 218 or 217 amino acids. Identity of the amino acid sequence of peroxiredoxins between *E. moshkovskii* and *E. histolytica* was considerably high (77–81%), but the N-terminus portion of *E. moshkovskii* peroxiredoxin was shorter than that of *E. histolytica*. A recombinant peroxiredoxin of *E. moshkovskii* expressed in *Escherichia coli* exhibited hydrogen peroxidase activity. Its K_m and V_{max} values of 35 μM and 0.07 μmol/min/mg protein were approximately 1 and 1.5 times greater than *E. histolytica* peroxiredoxin, respectively. In addition, the protective effect of *E. moshkovskii* peroxiredoxin against oxidative-nicking of supercoiled plasmid DNA was shown to be greater than that of *E. histolytica* peroxiredoxin. Confocal laser scanning microscopy, using polyclonal antibody against the recombinant *E. moshkovskii* peroxiredoxin, demonstrated that this protein was localized in the nucleus and cytoplasm of trophozoites, supporting its function as a protectant against DNA damage. Southern blot and real-time reverse transcription PCR analyses of the *E. moshkovskii* peroxiredoxin gene demonstrated that it was a multi-copy gene and its expression was comparable to that of *E. histolytica*. These results suggest that the antioxidant peroxiredoxin is important for protection against endogenously generated hydrogen peroxide in the nonpathogenic ameba.

Keywords: Antioxidant; Peroxiredoxin; *Entamoeba moshkovskii*; *Entamoeba histolytica*

1. Introduction

It has been proposed recently that peroxiredoxin (Prx) is an antioxidant enzyme family that includes thioredoxin peroxidase and alkyl hydroperoxidase [1]. The protein is ubiquitously distributed in a variety of prokaryotic and eukaryotic species, and has been implicated in a wide variety of cellular processes including proliferation, differentiation, and the immune response as well as the detoxification of peroxides [2–6]. Two-Cys Prx and 1-Cys Prx can be distinguished by the occurrence of one or two redox active site VCP motifs.

The genes coding 2-Cys Prx of the protozoan parasite, *Entamoeba histolytica*, a causative agent of human amebiasis, have been cloned in several laboratories [7–10]. The antioxidant activity of Prx, such as an elimination of H_2O_2, has been confirmed in both native and recombinant pro-

Abbreviations: DTT, dithiothreitol; HRP, horseradish peroxidase; MCO, metal-ion-catalyzed oxidation; ORF, open reading frame; PBS, phosphate-buffered saline; Prx, peroxiredoxin; SDS-PAGE, sodium dodecyl-sulfate polyacrylamide gel electrophoresis

☆ *Note:* Nucleotide sequence data reported in this paper are available in the DDBJ, EMBL, and GenBank™ databases under the accession numbers AB178086, AB178087, and AB178088.

* Corresponding author. Tel.: +81 463 93 1121; fax: +81 463 95 5450.
E-mail address: htachiba@is.icc.u-tokai.ac.jp (H. Tachibana).

0166-6851/$ – see front matter © 2004 Elsevier B.V. All rights reserved.
doi:10.1016/j.molbiopara.2004.08.009

teins [11,12]. Since there is no detectable catalase in *E. histolytica*, the *E. histolytica* Prx is considered to be important for protection from oxidative attack by activated host phagocytic cells during the ameba's invasion into host tissue and also to be important for protection against its own metabolically produced H_2O_2. The main difference in Prx between *E. histolytica* and other family members is an extended cysteine-rich N-terminal region present in *E. histolytica*. Interestingly, it has been demonstrated that a truncated form of *E. histolytica* Prx with a deletion of the cysteine-rich N-terminus region, showed a decreased level of H_2O_2 elimination compared with the native form [11]. Homologues of the *E. histolytica Prx* gene have also been cloned from the noninvasive parasitic ameba, *Entamoeba dispar*, which is morphologically indistinguishable from *E. histolytica* [13]. *E. dispar* Prx contains insertions of one, two or three repeats of YC(C/K)KE in the cysteine-rich N-terminus as compared to *E. histolytica*, although the role of these insertions has not yet been clarified. Difficulties encountered in the axenic cultivation of *E. dispar* may limit the comparative analysis of native Prx in nonpathogenic ameba.

Entamoeba moshkovskii is also morphologically indistinguishable from *E. histolytica* and *E. dispar*, but is usually isolated from the sediments of sewage-polluted waters [14]. One of the *E. moshkovskii* strains, Laredo, isolated from a human, was cultured successfully in the axenic medium developed for *E. histolytica* [15,16]. When *E. moshkovskii* genomic DNA was PCR amplified by primer pairs for *E. histolytica Prx* gene, some pairs were successfully used to yield PCR products, indicating that *Prx* gene is present in the nonpathogenic ameba but its sequence is not fully matched to that in *E. histolytica* [8]. As a step towards clarifying the biological significance of Prx in both pathogenic and nonpathogenic *Entamoeba*, we performed the molecular cloning and characterization of the *E. moshkovskii* Prx. Expression level, enzyme activity, and localization of the *E. moshkovskii* Prx were examined and compared with the Prx of *E. histolytica*. Uncovering the molecular characterization of Prxs in both pathogenic and nonpathogenic *Entamoeba* will ultimately allow us to sort out the functional significance of the molecules.

2. Materials and methods

2.1. Cultivation of parasites

Trophozoites of *E. moshkovskii* Laredo and *E. histolytica* HM-1:IMSS were axenically cultured in BI-S-33 medium [17] supplemented with 10% adult bovine serum at 25 and 37 °C, respectively. Trophozoites were harvested in the logarithmic phase of growth and were used in the following experiments.

2.2. Construction of the cDNA library and cloning of the Prx gene

Poly(A) RNA of *E. moshkovskii* trophozoites was isolated by the QuickPrep mRNA purification kit (Amersham). A cDNA library of *E. moshkovskii* was constructed from 3 μg of poly(A) RNA using a cDNA synthesis kit (Amersham) and a λgt11 vector kit (Stratagene). The library was screened with a 352-bp probe using the Gene Images AlkPhos Direct Labeling and Detection System (Amersham). The probe was prepared from genomic DNA by PCR amplification using primers p1 (5′-TAAAGCACCAGCATATTGTC-3′) and p3 (5′-GATGACATATCCTCTTCTTG-3′) which were derived from *Prx* gene of *E. histolytica*, as previously reported [8]. Positive clones were subcloned into a pUC19 vector and then sequenced. To extend the sequence of the 5′ end, rapid amplification of the cDNA end was performed with a 5′-Full RACE Core Set (Takara).

2.3. Southern and Northern blots analyses

Genomic DNA was isolated from *E. moshkovskii* trophozoites as described previously [8]. Three micrograms of the genomic DNA were digested with restriction enzymes including *Rsa*I, *Msp*I, *Hin*dIII and *Hin*fI. The fragments were separated on a 1% agarose gel, transferred to Hybond N^+ membrane (Amersham) by capillary action, and fixed by alkali-denaturation. The membrane was hybridized at 55 °C in a buffer containing the Gene Images AlkPhos Direct-labeled probe (Amersham) that was prepared by PCR amplification of a cloned cDNA using EHM30-1S (5′-GTATTGTTGTTTTATCCATT-3′) and EHM30-2AS (5′-CTTCCAATTCCATCATCATT-3′) as the primers. The membrane was treated with CDP-star detection reagent (Amersham) and then exposed to autoradiography films to detect the blots. Poly(A) RNA of *E. histolytica* trophozoites was also isolated by the QuickPrep mRNA purification kit. Three μg each of *E. moshkovskii* and *E. histolytica* poly(A) RNA were electrophoresed on a 1.2% formaldehyde-containing agarose gel. Blotting and hybridization were performed as described above. PCR products, prepared from a previously cloned cDNA coding *E. histolytica* Prx using primers EHM30-1S and EHM30-2AS, were also used as probes. The amino acid sequence deduced from the nucleotide sequence of the cDNA was identical to that of the *E. histolytica* Prx reported by Bruchhaus and Tannich [10].

2.4. Real-time reverse transcription PCR analysis

Total RNAs of *E. moshkovskii* and *E. histolytica* trophozoites were isolated using RNeasy mini kit (Qiagen) and used for cDNA synthesis in a GeneAmp RNA PCR kit (Applied Biosystems). A reaction mixture containing SYBR *Premix Ex Taq* (Takara), specific primers, and the cDNAs, was used for quantitative real-time PCR analysis. The primer pairs used were as follows; EmhPrx-S306 (5′-

TTGTCATCAAGCATGGTGTG-3′) and EmhPrx-AS518 (5′-GTTGATCTTCCAATTCCATCA-3′) for *Prx* genes, and EhmAct-S2 (5′-TTATGAAGGATTCTCACTTCC-3′) and EhmAct-AS2 (5′-TATCTCTGACAATTTCTCTTTC-3′) for actin genes. Forty cycles of amplification and the record of fluorescence intensity in each cycle were performed by the ABI PRISM 7700 Sequence Detection System (Applied Biosystems). After initial denaturation at 95 °C for 10 s, a shuttle PCR protocol consisting of denaturation at 95 °C for 5 s and annealing-extension at 60 °C for 30 s was applied. PCR end products were subjected to agarose gel electrophoresis to test the specificity of each amplification. Relative quantitation of data from the ABI PRISM 7700 Sequence Detection System software version 1.7 was performed by the comparative C_T method using actin genes as internal standards. Experiments including the culturing of trophozoites and isolation of RNA were repeated three times.

2.5. Expression and purification of recombinant Prxs

One of the cloned cDNAs encoding *E. moshkovskii* Prx was amplified by PCR. A recognition site for *Nde*I was added to the forward primer (5′-CCCATATGA-GTTGCACAAAACAATGTTG-3′) and a recognition site for *Bam*HI was added to the reverse primer (5′-CCGGATCCAATTAATGAGAAGATAAATACT-3′). After digestion with these restriction enzymes, the DNA fragment was ligated with expression vector pET19b (Novagen) and introduced *into Escherichia coli* BL21(DE3)pLysS by transformation. The expression of recombinant Prx tagged with histidine residues was induced with 1 mM isopropyl-β-D-thiogalactopyranoside. The protein was purified by affinity chromatography using His-Bind Resin (Novagen) according to the manufacturer's recommendations. The eluted protein was dialyzed against 10 mM phosphate-buffered saline, pH 7.2 (PBS), and analyzed by sodium dodecyl sulfate-polyacrylamide gel electrophoresis (SDS-PAGE) using a 10% gel under reducing conditions [18]. As a control, the recombinant Prx of *E. histolyytica* was also prepared as above. Primers (5′-CCCATATGTCTTGCAATCAACAAAAAGAGT-3′) and (5′-CCGGATCCTTTTAATGTGCTGTTAAATATT-3′) were used for the amplification of the cDNA coding *E. histolytica* Prx.

2.6. Preparation of polyclonal antibodies and western immunoblot analysis

Purified recombinant Prx was injected intraperitoneally into three Chinese hamsters. The first injection was in complete Freund's adjuvant, thereafter followed with two injections in incomplete Freund's adjuvant at intervals of 2 weeks. One week after the last injection, sera of the hamsters were collected. Crude proteins of *E. moshkovskii* trophozoites were solubilized by suspending the cells in lysis buffer [18] containing 2 mM phenylmethylsulfonyl fluoride, 2 mM *N* α-*p*-tosyl-L-lysine choromethyl ketone, 2 mM *p*-hydroxymercuriphenyl sulfonic acid, and 4 μM leupeptin with 10% 2-mercaptoethanol, and then heating at 95 °C for 5 min. These proteins were separated by SDS-PAGE using 10% gel under reducing conditions. After electrophoresis, the protein bands were transferred onto a polyvinylidene difluoride membrane by semi-dry electroblotting, blocked with 3% skim-milk in PBS, and then incubated with the anti-Prx hamster sera (1:200 dilution). Horseradish peroxidase (HRP) conjugated goat IgG to hamster IgG (ICN Pharmaceuticals) was used as a secondary antibody. The reaction was visualized with a Konica Immunostaining HRP-1000 kit.

2.7. Confocal microscopy

E. moshkovskii trophozoites were transferred onto glass coverslips in a culture dish containing BI-S-33 medium supplemented with 10% adult bovine serum and incubated for 2 h at 25 °C. After discarding the medium, the coverslips were incubated in 4% paraformaldehyde in PBS for 30 min. After washing with PBS, the trophozoites were permealized with 0.1% Triton X-100 for 5 min at room temperature. Cells were washed with PBS and then blocked with 3% bovine serum albumin in PBS for 1 h at room temperature. Anti-Prx hamster sera (1:100 dilution) was added and the cells were incubated for an additional 12 h at 4 °C. The coverslips were washed with PBS and then incubated with fluorescein isothiocyanate-conjugated goat IgG to hamster IgG (ICN Pharmaceuticals) for 5 h at 4 °C. The coverslips were again washed with PBS, stained by 2.5 μg/ml propidium iodide for 10 min at room temperature and then mounted. The samples were observed by a Zeiss LM410 confocal laser scanning microscope.

2.8. Metal-catalyzed oxidation assay

This assay measures the ability of the recombinant Prx to protect a supercoiled plasmid being nicked by a metal-ion-catalyzed oxidation (MCO) system consisting of Fe^{3+}, O_2 and an electron donor dithiothreitol (DTT) [19]. The reaction was monitored in mixtures containing 500 ng of pUC19 plasmid DNA, 60 μM $FeCl_3$, 10 mM DTT, 100 μM EDTA, and various concentrations of recombinant Prx. The mixtures were incubated for 30 min, 1, 2 and 4 h, respectively, and then the plasmid DNA was subjected to agarose gel electrophoresis and stained with ethidium bromide. Densitometry scans were obtained using a Cool Saver AE6955 (Atto) and analyzed by CS analyzer software (Atto).

2.9. Assay for enzyme activity

The enzyme activity of recombinant Prx was measured as described by Chandrashekar et al. [20]. The reaction mixture, containing 1 mM DTT, 100 μM H_2O_2, and various amounts of recombinant Prx in 100 mM sodium phosphate buffer (pH 7.0), was incubated at 37 °C for 20 min. The reaction was

quenched by adding trichloroacetic acid to a final concentration of 10%. The mixture was centrifuged to remove the precipitate and the supernatant mixed with ferrous ammonium sulfate and potassium thiocyanate. The peroxide amounts in this mixture were estimated from its optical density at 480 nm. The background of the mixture containing no recombinant Prx was subtracted from these values.

In order to determine the kinetic parameters of enzyme activity (K_m and V_{max}), we determined the reaction rates by changing the concentrations of H_2O_2. A mixture containing recombinant Prx, 1 mM DTT, and 100 mM sodium phosphate, pH 7.0 was preincubated at 25 °C for 10 min and then incubated at 37 °C for 20 min after adding various amounts of H_2O_2. The reaction rates were plotted against the concentration of H_2O_2 in a double reciprocal manner to determine K_m and V_{max}.

3. Results

3.1. Cloning of cDNAs encoding E. moshkovskii Prx

The open reading frame (ORF) of three cloned cDNAs encoded a polypeptide of 218 (clone 1) or 217 (clones 2 and 3) amino acids (Fig. 1A). The calculated molecular masses and theoretical p*I* were 24,484 Da and 6.57 in clone 1; 24,377 Da and 7.02 in clone 2; and 24,410 Da and 6.57 in clone 3. When the deduced amino acid sequences of these Prxs were compared by the BLAST 2 program, identities were 98.6% between clones 1 and 2, 94.5% between clones 1 and 3, and 94.9% between clones 2 and 3. The amino acid sequences of the *E. moshkovskii* Prxs were also compared with the Prx of *E. histolytica* (233 amino acids). The identities of the *E. moshkovskii* Prx clones 1–3 with the *E. histolytica* Prx were 79.6, 80.9 and 76.7%, respectively. The two active site VCP motifs essential for the activity of 2-Cys Prx were conserved in the three clones. A distinctive difference was that the N-terminus sequence of the *E. moshkovskii* Prx was shorter than that of the *E. histolytica* Prx.

A search of the *E. moshkovskii* genomic sequences available on the Sanger Institute website (http://www.sanger.ac.uk/Projects/E_moshkovskii/) was performed although the project is incomplete and not yet assembled. The strain being studied in the genome project is the FIC strain which was isolated from sewage in Canada. The TBLASTN search using the 3 Prx sequences identified 28 putative ORFs. When the search was extended to uncover

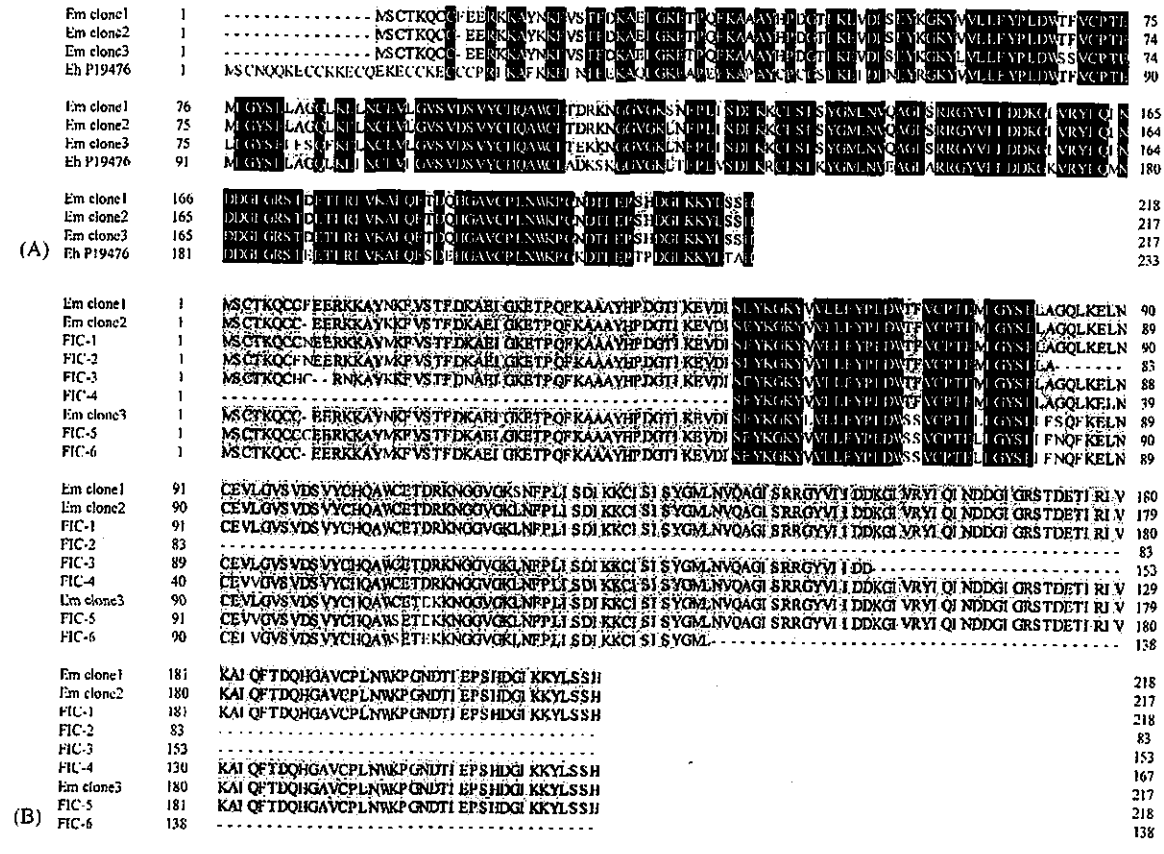

Fig. 1. (A) Alignment of deduced amino acid sequences of three Prx cDNA clones from *E. moshkovskii* and *E. histolytica* Prx (P19476). Identical and conserved amino acid residues are highlighted in black and gray, respectively. (B) Alignment of deduced amino acid sequences of the three Prx cDNA clones from *E. moshkovskii* and six unique open reading frames (FIC-1 to -6) from an *E. moshkovskii* genome database. Sequence numbers in the database are as follows: FIC-1, mosh045g12.p1k and mosh045g12.q1k; FIC-2, mosh042a08.p1k; FIC-3, mosh043g08.q1k; FIC-4, mosh002c07.q1k; FIC-5, mosh019g11.p1k and mosh019g11.q1k; FIC-6, mosh086a01.q1k.

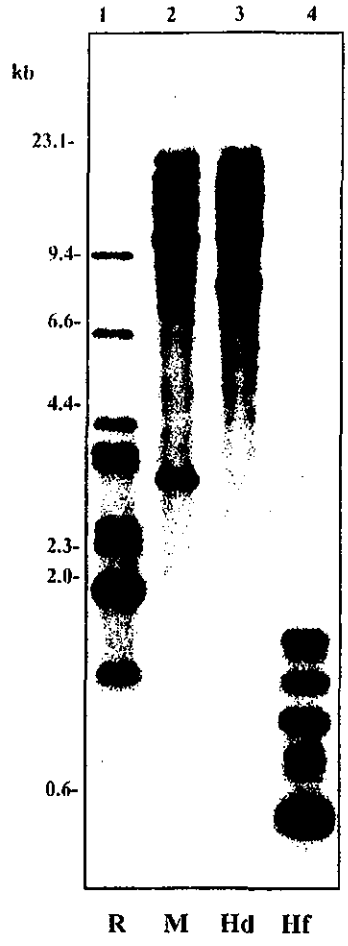

Fig. 2. Southern blot analysis of *Prx* genes in *E. moshkovskii*. Genomic DNA was digested with *Rsa*I (R, lane 1), *Msp*I (M, lane 2), *Hin*dIII (Hd, lane 3), and *Hin*fI (Hf, lane 4) and hybridized with a probe. Numbers to the left indicate DNA sizes of markers (in kilobases).

sequences with higher homology (e values of $1.1e^{-108}$ to $1.9e^{-36}$), at least six unique ORFs were identified (Fig. 1B). Of these, four ORFs showed higher homology with clones 1 and 2, whereas the other two ORFs were similar with clone 3. However, none of the six ORFs showed complete homology with the three *Prx* genes from the Laredo strain, suggesting the presence of sequence differences in the *Prx* genes of these strains.

3.2. Southern blot analysis of the Prx genes

PCR amplification of cDNA clone 1, using primers EHM30-1S and EHM30-2AS, yielded 335-bp products. A Southern blot hybridization, using the PCR product as a probe, was performed on *E. moshkovskii* genomic DNA digested with *Rsa*I, *Msp*I, *Hin*dIII, and *Hin*fI (Fig. 2). The hybridization pattern revealed that the Prx is part of a multigene family. The pattern of digestion by *Rsa*I demonstrated that at least nine *Prx* genes were existing in the genomic DNA.

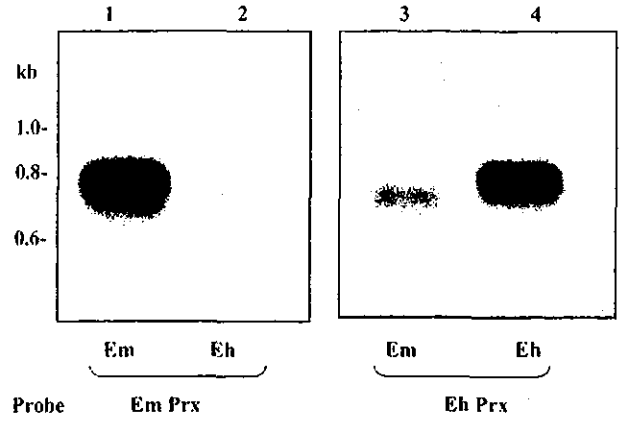

Fig. 3. Northern blot analyses of *Prx* genes in *E. moshkovskii* (Em, lanes 1 and 3) and *E. histolytica* (Eh, lanes 2 and 4). Hybridizations using probes specific for *E. moshkovskii* (Em Prx, lanes 1 and 2) and specific for *E. histolytica* (Eh Prx, lanes 3 and 4) were performed. Numbers to the left indicate the size of RNA markers (in kilobases).

3.3. Northern blot and real-time reverse transcription PCR analyses of Prx genes

To compare the expression profiles of *Prx* genes between *E. moshkovskii* and *E. histolytica*, Northern blot analysis was performed using two probes prepared from the two species of ameba (Fig. 3). Difference in nucleotide sequences between two probes was 12% in 335 bp. Single bands of 0.75 and 0.8 kb were detected in *E. moshkovskii* and *E. histolytica*, respectively. To measure quantitatively the expression of the *Prx* genes in both species, real-time reverse transcription PCR was performed and the results analyzed by a comparative C_T method using actin genes as internal standards. In experiments repeated in triplicate, the relative expression levels of *E. moshkovskii* Prx to *E. histolytica* Prx were estimated to be 0.98, 1.37, and 0.83, respectively. The mean value of 1.06 ± 0.28 indicates that the *Prx* gene expression is comparable between the two species.

3.4. Expression and purification of recombinant Prxs

The Prxs of *E. moshkovskii* (clone 1) and *E. histolytica* were expressed in *E. coli* and purified by affinity chromatography. SDS-PAGE showed the proteins of *E. moshkovskii* and *E. histolytica* to be highly homogeneous with molecular masses estimated at 27 and 31 kDa, respectively, under reducing conditions (lanes 3 and 6 of Fig. 4). The yield of recombinant proteins was approximately 60 mg/l of bacterial culture.

3.5. Identification and localization of native Prx in E. moshkovskii

To determine the localization of the native Prx in *E. moshkovskii*, a polyclonal antibody against recombinant Prx was prepared in hamsters. In Western immunoblot analysis, the antibody was reactive with a 25-kDa band of *E.*

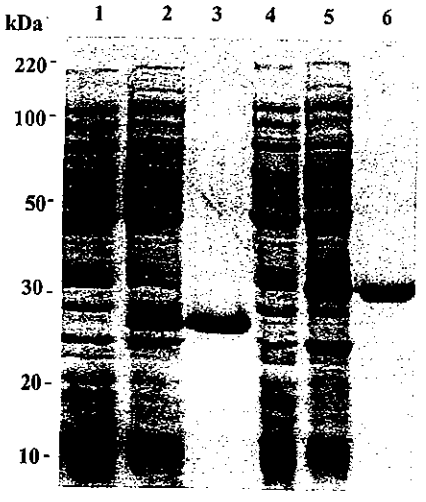

Fig. 4. SDS-PAGE of the recombinant Prxs of *E. moshkovskii* (lanes 1–3) and *E. histolytica* (lanes 4–6) expressed in *E. coli*. Bacterial lysates or purified Prxs were run in a 10% gel under reducing conditions and were stained with Coomassie brilliant blue. Lanes 1 and 4, *E. coli* lysates without induction; lanes 2 and 5, *E. coli* lysates after induction with isopropyl-β-D-thiogalactopyranoside; lanes 3 and 6, purified Prxs. Numbers to the left indicate molecular masses of size markers (in kilodaltons).

moshkovskii, under reduced conditions (Fig. 5). A faintly stained 45-kDa band was also detected, probably a dimeric form of Prx. The antibody also recognized a 30-kDa antigen of *E. histolytica* trophozoites, but reactivity was much lower.

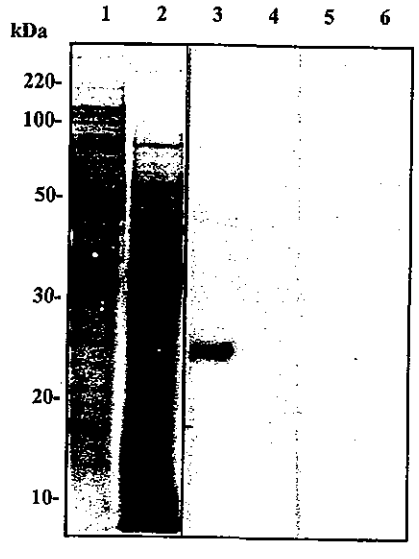

Fig. 5. Western immunoblot of the native Prx of *E. moshkovskii*. Lysates of *E. moskovskii* (lanes 1, 3 and 5) and *E. histolytica* trophozoites (lanes 2, 4 and 6) were subjected to SDS-PAGE in a 10% gel under reducing conditions and then transferred to polyvinylidene difluoride membranes. Protein bands of lanes 1 and 2 were stained with Coomassie brilliant blue. Lanes 3 and 4 were treated with sera of hamsters immunized with the recombinant Prx of *E. moshkovskii*; lanes 5 and 6 were treated with the preimmune sera of the hamsters. HRP-conjugated goat antibody to hamster IgG was used as a secondary antibody. Numbers to the left indicate molecular masses of size markers (in kilodaltons).

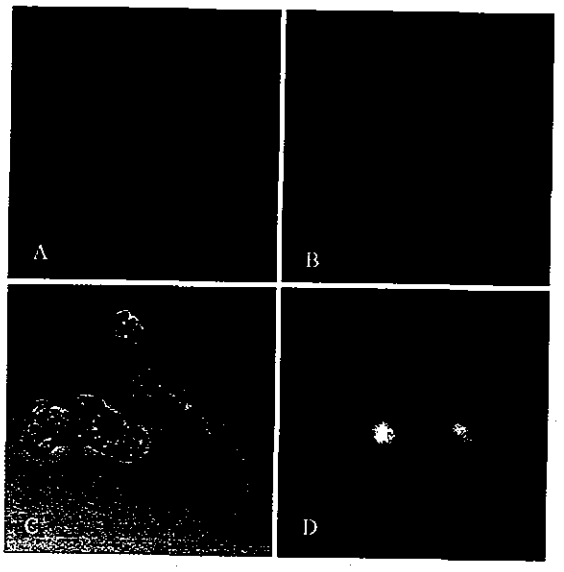

Fig. 6. Localization of Prx in *E. moshkovskii* trophozoites observed by confocal laser scanning microscopy. (A) staining with a polyclonal antibody to the Prx. Bright fluorescence was located in the nucleus and cytoplasm of trophozoites. (B) Nuclear staining with propidium iodide. (C) Differential interference contrast microscopy. (D) Merger of A, B and C. Bar indicates 10 μm.

This suggests that antigenicity of *E. moshkovskii* Prx is significantly different from the *E. histolytica* Prxs or that there is much less Prx in *E. histolytica* than in *E. moshkovskii*.

Confocal laser scanning microscopy, using the polyclonal antibody against *E. moshkovskii* Prx, clearly showed the intracellular localization of Prx in the *E. moshkovskii* trophozoites; more specifically, bright fluorescences were observed in the nucleus and cytoplasm of the trophozoites (Fig. 6).

3.6. Protection of supercoiled DNA from oxidative damage by Prx

The nicks of supercoiled DNA are formed by oxidative radicals such as those generated by the metal-ion-catalyzed oxidation (MCO) system. Since the nick formation of DNA is easily detectable, as seen in lane 3 of Fig. 7, Prx was tested for its ability to protect supercoiled DNA from degradation by the MCO system. When plasmid DNA was mixed and incubated with the various concentrations of Prx, the amounts of the nicked form of plasmid DNA decreased as Prx increased (Fig. 7A), demonstrating that Prx possesses protective activity against oxidative radicals. Densitometric analysis of the gel demonstrated that the protective effect of the *E. moshkovskii* Prx appeared to be greater than that of *E. histolytica* Prx, at 0.5 and 0.1 μM of protein (Fig. 7B).

3.7. Antioxidant activity of the Prx

The antioxidant activity of the recombinant Prx of *E. moshkovskii* was examined by measuring its ability to remove H_2O_2 in the ferrithiocyanate assay. The *E. moshkovskii* Prx catalyzed the removal of H_2O_2 in the presence of DTT

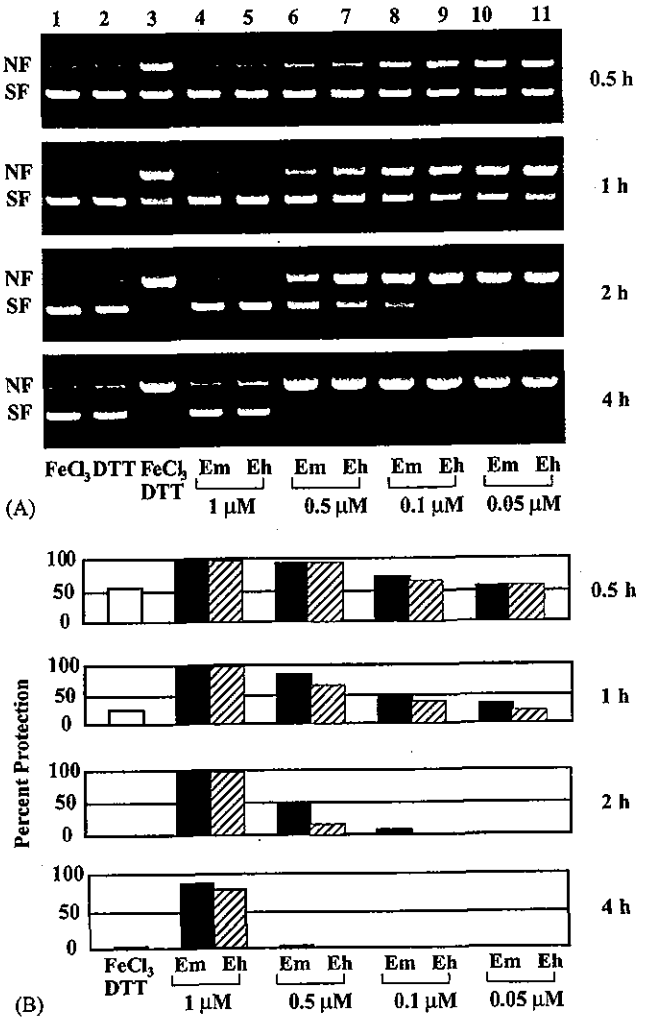

Fig. 7. Protection of DNA cleavage by the recombinant Prxs of *E. moshkovskii* and *E. histolytica*. (A) Agarose gel separation of nicked form (NF) and supercoiled form (SF). A mixture containing supercoiled pUC19 plasmid DNA (500 ng per lane), components of the metal-catalyzed oxidation (MCO) system (16.5 μM $FeCl_3$ and 3.3 mM DTT), and various concentrations of Prx were incubated for 0.5–4 h and then electrophoresed in a 1% agarose gel. Lane 1, $FeCl_3$; lane 2, DTT; lane 3, $FeCl_3$ and DTT; lanes 4, 6, 8 and 10, $FeCl_3$, DTT and 1, 0.5, 0.1 and 0.05 μM *E. moshkovskii* Prx (Em), respectively; lanes 5, 7, 9 and 11, $FeCl_3$, DTT and 1, 0.5, 0.1 and 0.05 μM *E. histolytica* Prx (Eh), respectively. (B) Densitometric analysis of the agarose gels (lanes 3–11 in A). Protection was expressed as a percentage of supercoiled form to the sum of supercoiled and nicked form.

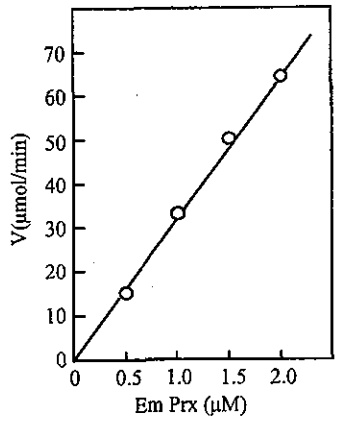

Fig. 8. Concentration dependency of recombinant Prx of *E. moshkovskii* on the reaction rate. A mixture containing *E. moshkovskii* Prx at the various concentrations in 1 mM DTT/100 mM sodium phosphate buffer, pH 7.0, was incubated at 25 °C for 10 min. The reaction was started by adding H_2O_2 (final concentration of 100 μM) to the mixture and incubating at 37 °C for 20 min. Next, the concentration of H_2O_2 was determined according to the method described by Chandrashekar et al. [20]. The reaction rates were plotted against the concentration of *E. moshkovkii* Prx.

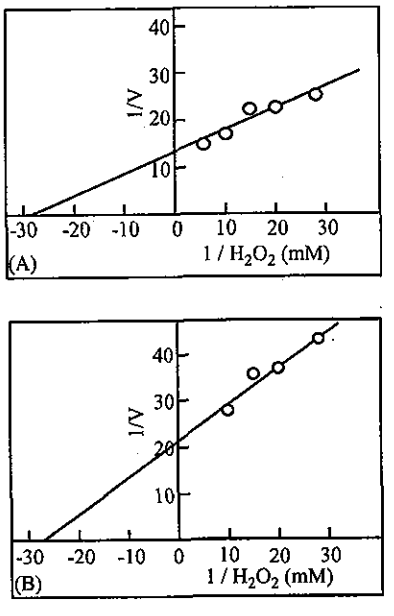

Fig. 9. The double reciprocal plots for the reaction of recombinant Prxs of *E. moshkovskii* (A) and *E. histolytica* (B). The mixture containing Prx, 1 mM DTT and 100 mM sodium phosphate, pH 7.0 was incubated at 25 °C for 10 min. The reaction was started by addition of various concentrations of H_2O_2 and incubating at 37 °C for 20 min. The reaction rates were plotted against the concentrations of H_2O_2 in a double reciprocal manner.

in a concentration-dependent manner (Fig. 8), demonstrating that this protein possesses antioxidant activity. Next, we examined Prx activity by changing the concentration of H_2O_2. The results gave the normal Michaelis–Menten pattern with K_m values of 35 and 36 μM, and V_{max} of 0.07 and 0.046 μmol/min/mg protein for H_2O_2 reduction in *E. moshkovskii* and *E. histolytica*, respectively (Fig. 9). These results indicate that the H_2O_2 detoxification activity of Prx is highly conserved in both pathogenic and nonpathogenic parasites.

4. Discussion

In the present study, a 2-Cys Prx from the nonpathogenic *E. moshkovskii* has been characterized and compared with a Prx from *E. histolytica*. Amino acid aligment between the *E. moshkovskii* and *E. histolytica* Prxs revealed that the *E. hitolytica* Prx has an extended N-terminus region compared with that of *E. moshkovskii*. Since it was shown that truncation of the cysteine-rich N-terminus region of 40 amino acid

residues from *E. histolytica* Prx decreased the H_2O_2 eliminating activity to one half the level of the native form [11], it was predicted that *E. moshkovskii* Prx would exhibit lower activity. However, there was no significant difference in the K_m values of the two species. Furthermore, V_{max} and the protective effect on DNA cleavage of the *E. moshkovskii* Prx were shown to be higher than those of the *E. histolytica* Prx. In addition, the expression level of the gene in *E. moshkovskii* was comparable with that of *E. histolytica* when both species were cultured in the same anaerobic medium. Therefore, it seems that Prx is an important antioxidant to metabolically generated H_2O_2 in the nonpathogenic ameba. As *E. moshkovskii* is primarily isolated from polluted water, it is considered to be a free-living ameba [14]. *E. moshkovskii* trophozoites can grow at room temperature whereas *E. histolytica* trophozoites cannot. Finding that the level of *E. moshkovskii Prx* gene expression at 25 °C is comparable to the Prx of *E. histolytica* at 37 °C suggests that sufficient Prx activity is maintained even at a lower temperature and may contribute to the survival and growth of the non-pathogenic ameba. The expression level of *Prx* genes seems to vary depending on the environmental conditions. Since the exposure of *E. histolytica* trophozoites to a higher oxygen concentration for 1 h caused a twofold higher expression of the Prx mRNA [21], the *E. moshkovskii* Prx might be expressed at higher levels under free-living conditions than under anaerobic conditions either in culture or on the epithelium of the human intestine. Interestingly, it has been demonstrated in *E. histolytica* that an increase in the expression of Prx is accompanied by metronidazole resistance [22]. Further studies are required to clarify the specific factors that influence the expression of *E. moshkovskii* Prx.

Localization of *E. moshkovskii* Prx in the nucleus and cytoplasm is in agreement with our previous observation on the localization of *E. histolytica* Prx [23]. To the contrary, Torian et al. [7] proposed that the Prx was localized on the surface of *E. histolytica*. Recently, it was shown that *E. histolytica* Prx was co-localized with the 260-kDa galactose- and *N*-acetyl-D-galactosamine-inhibitable (Gal/GalNAc) surface lectin in *E. histolytica* trophozoites [24]. The reason why distinctly different localizations of *E. histolytica* Prx were observed in different laboratories is not yet clear. In mammals, six subclasses of Prx, Prx I–VI, have been identified and the cellular localization of these proteins has been demonstrated: Prx I in the cytosol and nucleus, Prx II in the cytosol and membrane, and Prx III in the mitochondria [6]. Nuclear localization has been demonstrated in one of five Prxs in *Saccharomyces cerevisiae* [25]. In the N-terminus sequences of *Entamoeba* Prxs, there are none corresponding to the signal sequences of mammalian Prx III, IV and V for mitochondrial import or secretion, or the sequences of yeast Prxs for mitochondrial or nuclear localization. However, since three different amino acids sequences of *E. moshkovskii* Prxs were identified in this study, we cannot rule out the possibility that there may be different localizations and functions among the Prxs. Indeed, in other protozoa such as *Leishmania* and *Plasmodium*, different functions of the 2-Cys and 1-Cys Prxs have been demonstrated [26–28], although 1-Cys Prx has not been detected as yet in *Entamoeba*. It is also possible that localization of the Prxs change, depending on culture conditions or some stimulation. For instance the interaction of *E. histolytica* trophozoites with host cells may stimulate the recruitment of Prx to the surface [24]. In any event, the localization of *Entamoeba* Prx in the nucleus in non-stimulated conditions is reasonable if the protection of DNA from oxidative stress is mediated by Prx.

Sporadic cases of human infection with the free-living ameba, *E. moshkovskii*, have been reported. Indeed, the *E. moshkovskii* strain, Laredo, used in the present study, was isolated from a human [15,16]. However, a high prevalence of *E. moshkovskii* infection was recently demonstrated in children in Bangladesh suggesting that humans may be a true host of the ameba [29]. The sequence differences of *Prx* genes between the Laredo and FIC strains suggest that human isolates may be different from environmental isolates. The possibility is supported by the observation that the PCR products of the Arg^{TCT} tRNA gene are quite dissimilar in size between the Laredo and FIC strains [29].

E. moshkovskii is morphologically indistinguishable from *E. histolytica* and the nonpathogenic *E. dispar*. Therefore, precise identification of the amebic species is important. We have previously demonstrated that *Prx* genes are available as a target for distinguishing between *E. histolytica* and *E. dispar* [8,13,30]. Indeed, PCR amplification of *Prx* genes has been applied to the laboratory diagnosis and field studies of amebiasis [31–36]. In the present study, we showed that there are some differences in nucleotide sequences between the *E. moshkovskii* and *E. histolytica*/*E. dispar Prx* genes. In addition, the *Prx* gene of *E. moshkovskii* was demonstrated to be a multi-copy gene. Therefore, we consider that DNA diagnosis can be useful for identifying *E. moshkovskii* by targeting its *Prx* genes.

Acknowledgements

We thank Drs. L.S. Diamond and S. Kobayashi for a generous supply of the axenic ameba strains. We also thank Dr. J. Itoh for his help with the confocal microscopy. This work was supported by a Grant-in-Aid for Scientific Research from the Japanese Society for the Promotion of Science, and a grant from the Ministry of Health, Labour and Welfare of Japan. X.-J.C. is a recipient of the Japanese Society for the Promotion of Science Postdoctoral Fellowship for Foreign Researchers.

References

[1] Chae HZ, Robison K, Poole LB, Church G, Storz G, Rhee SG. Cloning and sequencing of thiol-specific antioxidant from mammalian brain: alkyl hydroperoxide reductase and thiol-specific antioxidant define a large family of antioxidant enzymes. Proc Natl Acad Sci USA 1994;91:7017–21.

[2] Henkle-Duhrsen K, Kampkotter A. Antioxidant enzyme families in parasitic nematodes. Mol Biochem Parasitol 2001;114:129–42.
[3] Fujii J, Ikeda Y. Advances in our understanding of peroxiredoxin, a multifunctional, mammalian redox protein. Redox Rep 2002;7:123–30.
[4] Hofmann B, Hecht HJ, Flohe L. Peroxiredoxins Biol Chem 2002;383:347–64.
[5] Dietz KJ. Plant peroxiredoxins. Annu Rev Plant Biol 2003;54:93–107.
[6] Wood ZA, Schroder E, Robin Harris J, Poole LB. Structure, mechanism and regulation of peroxiredoxins. Trends Biochem Sci 2003;28:32–40.
[7] Torian BE, Flores BM, Strocher VL, Hagen FS, Stamm WE. cDNA sequence analysis of a 29-kDa cysteine-rich surface antigen of pathogenic *Entamoeba histolytica*. Proc Natl Acad Sci USA 1990;87:6358–62.
[8] Tachibana H, Ihara S, Kobayashi S, Kaneda Y, Takeuchi T, Watanabe Y. Differences in genomic DNA sequences between pathogenic and nonpathogenic isolates of *Entamoeba histolytica* identified by polymerase chain reaction. J Clin Microbiol 1991;29:2234–9.
[9] Reed SL, Flores BM, Batzer MA, et al. Molecular and cellular characterization of the 29-kDa peripheral membrane protein of *Entamoeba histolytica*: differentiation between pathogenic and nonpathogenic isolates. Infect Immun 1992;60:542–9.
[10] Bruchhaus I, Tannich E. Analysis of the genomic sequence encoding the 29-kDa cysteine-rich protein of *Entamoeba histolytica*. Trop Med Parasitol 1993;44:116–8.
[11] Bruchhaus I, Richter S, Tannich E. Removal of hydrogen peroxide by the 29 kDa protein of *Entamoeba histolytica*. Biochem J 1997;326:785–9.
[12] Poole LB, Chae HZ, Flores BM, Reed SL, Rhee SG, Torian BE. Peroxidase activity of a TSA-like antioxidant protein from a pathogenic amoeba. Free Radic Biol Med 1997;23:955–9.
[13] Tachibana H, Cheng XJ. *Entamoeba dispar*: cloning and characterization of peroxiredoxin genes. Exp Parasitol 2000;94:51–5.
[14] Scaglia M, Gatti S, Strosselli M, Grazioli V, Villa MR. *Entamoeba moshkovskii* (Tshalaia, 1941): morpho-biological characterization of new strains isolated from the environment, and a review of the literature. Ann Parasitol Hum Comp 1983;58:413–22.
[15] Dreyer DA. Growth of a strain of *Entamoeba histolytica* at room temperature. Tex Rep Biol Med 1961;19:393–6.
[16] Clark CG, Diamond LS. The Laredo strain and other '*Entamoeba histolytica*-like' amoebae are *Entamoeba moshkovskii*. Mol Biochem Parasitol 1991;46:11–8.
[17] Diamond LS, Harlow DR, Cunnick CC. A new medium for the axenic cultivation of *Entamoeba histolytica* and other Entamoeba. Trans R Soc Trop Med Hyg 1978;72:431–2.
[18] Laemmli UK. Cleavage of structural proteins during the assembly of the head of bacteriophage T4. Nature 1970;227:680–5.
[19] Lim YS, Cha MK, Kim HK, et al. Removals of hydrogen peroxide and hydroxyl radical by thiol-specific antioxidant protein as a possible role in vivo. Biochem Biophys Res Commun 1993;192:273–80.
[20] Chandrashekar R, Tsuji N, Morales TH, et al. Removal of hydrogen peroxide by a 1-cysteine peroxiredoxin enzyme of the filarial parasite *Dirofilaria immitis*. Parasitol Res 2000;86:200–6.
[21] Akbar MA, Chatterjee NS, Sen P, et al. Genes induced by a high-oxygen environment in *Entamoeba histolytica*. Mol Biochem Parasitol 2004;133:187–96.
[22] Wassmann C, Hellberg A, Tannich E, Bruchhaus I. Metronidazole resistance in the protozoan parasite *Entamoeba histolytica* is associated with increased expression of iron-containing superoxide dismutase and peroxiredoxin and decreased expression of ferredoxin 1 and flavin reductase. J Biol Chem 1999;274:26051–6.
[23] Tachibana H, Kobayashi S, Kato Y, Nagakura K, Kaneda Y, Takeuchi T. Identification of a pathogenic isolate-specific 30,000-Mr antigen of *Entamoeba histolytica* by using a monoclonal antibody. Infect Immun 1990;58:955–60.
[24] Hughes MA, Lee CW, Holm CF, et al. Identification of *Entamoeba histolytica* thiol-specific antioxidant as a GalNAc lectin-associated protein. Mol Biochem Parasitol 2003;127:113–20.
[25] Park SG, Cha MK, Jeong W, Kim IH. Distinct physiological functions of thiol peroxidase isoenzymes in *Saccharomyces cerevisiae*. J Biol Chem 2000;275:5723–32.
[26] Barr SD, Gedamu L. Cloning and characterization of three differentially expressed peroxidoxin genes from *Leishmania chagasi*. Evidence for an enzymatic detoxification of hydroxyl radicals. J Biol Chem 2001;276:34279–87.
[27] Barr SD, Gedamu L. Role of peroxidoxins in *Leishmania chagasi* survival. Evidence of an enzymatic defense against nitrosative stress. J Biol Chem 2003;278:10816–23.
[28] Kawazu S, Nozaki T, Tsuboi T, et al. Expression profiles of peroxiredoxin proteins of the rodent malaria parasite *Plasmodium yoelii*. Int J Parasitol 2003;33:1455–61.
[29] Ali IK, Hossain MB, Roy S, et al. *Entamoeba moshkovskii* infections in children, Bangladesh. Emerg Infect Dis 2003;9:580–4.
[30] Tachibana H, Kobayashi S, Takekoshi M, Ihara S. Distinguishing pathogenic isolates of *Entamoeba histolytica* by polymerase chain reaction. J Infect Dis 1991;164:825–6.
[31] Tachibana H, Kobayashi S, Paz KC, Aca IS, Tateno S, Ihara S. Analysis of pathogenicity by restriction-endonuclease digestion of amplified genomic DNA of *Entamoeba histolytica* isolated in Pernambuco, Brazil. Parasitol Res 1992;78:433–6.
[32] Tachibana H, Kobayashi S, Okuzawa E, Masuda G. Detection of pathogenic *Entamoeba histolytica* DNA in liver abscess fluid by polymerase chain reaction. Int J Parasitol 1992;22:1193–6.
[33] Ohnishi K, Murata M, Kojima H, Takemura N, Tsuchida T, Tachibana H. Brain abscess due to infection with *Entamoeba histolytica*. Am J Trop Med Hyg 1994;51:180–2.
[34] Rivera WL, Tachibana H, Kanbara H. Field study on the distribution of *Entamoeba histolytica* and *Entamoeba dispar* in the northern Philippines as detected by the polymerase chain reaction. Am J Trop Med Hyg 1998;59:916–21.
[35] Tachibana H, Kobayashi S, Nagakura K, Kaneda Y, Takeuchi T. Asymptomatic cyst passers of *Entamoeba histolytica* but not *Entamoeba dispar* in institutions for the mentally retarded in Japan. Parasitol Int 2000;49:31–5.
[36] Pinheiro SM, Carneiro RM, Aca IS, et al. Determination of the prevalence of *Entamoeba histolytica* and *E. dispar* in the pernambuco state of northeastern Brazil by a polymerase chain reaction. Am J Trop Med Hyg 2004;70:221–4.

THE JOURNAL OF BIOLOGICAL CHEMISTRY
Vol. 279, No. 3, Issue of January 16, pp. 2316–2323, 2004
Printed in U.S.A.

Molecular Cloning and Characterization of a Protein Farnesyltransferase from the Enteric Protozoan Parasite *Entamoeba histolytica**

Received for publication, October 20, 2003
Published, JBC Papers in Press, October 28, 2003, DOI 10.1074/jbc.M311478200

Masahiro Kumagai‡, Asao Makioka‡, Tsutomu Takeuchi§, and Tomoyoshi Nozaki¶‖**

From the ‡Department of Tropical Medicine, Jikei University School of Medicine, 3-25-8 Nishi-shinbashi, Minato-ku, Tokyo 105-8461, Japan, the §Department of Tropical Medicine and Parasitology, Keio University School of Medicine, 35 Shinanomachi, Shinjuku-ku, Tokyo 160-8582, Japan, the ¶Department of Parasitology, National Institute of Infectious Diseases, 1-23-1 Toyama, Shinjuku-ku, Tokyo 162-8640, Japan, and the ‖Precursory Research for Embryonic Science and Technology, Japan Science and Technology Agency, 2-20-5 Akebonocho, Tachikawa, Tokyo 190-0012, Japan

Genes encoding α- and β-subunits of a putative protein farnesyltransferase (FT) from the enteric protozoan parasite *Entamoeba histolytica* were obtained and their biochemical properties were characterized. Deduced amino acid sequences of the α- and β-subunit of *E. histolytica* FT (*Eh*FT) were 298- and 375-residues long with a molecular mass of 35.6 and 42.6 kDa, and a pI of 5.43 and 5.65, respectively. They showed 24% to 36% identity to and shared common signature domains and repeats with those from other organisms. Recombinant α- and β-subunits, co-expressed in *Escherichia coli*, formed a heterodimer and showed activity to transfer farnesyl using farnesylpyrophosphate as a donor to human H-Ras possessing a C-terminal CVLS, but not a mutant H-Ras possessing CVLL. Among a number of small GTPases that belong to the Ras superfamily from this parasite, we identified *Eh*Ras4, which possesses CVVA at the C terminus, as a sole farnesyl acceptor for *Eh*FT. This is in contrast to mammalian FT, which utilizes a variety of small GTPases that possess a C-terminal C*aaX* motif, where *X* is serine, methionine, glutamine, cysteine, or alanine. *Eh*FT also showed remarkable resistance against a variety of known inhibitors of mammalian FT. These results suggest that remarkable biochemical differences in binding to substrates and inhibitors exist between amebic and mammalian FTs, which highlights this enzyme as a novel target for the development of new chemotherapeutics against amebiasis.

Ras small GTPases function as a molecular switch of signal transduction in cell proliferation and differentiation (1). Ras small GTPases require a post-translational lipid modification called protein farnesylation in order to become membrane-associated and functional (2). Protein farnesylation, catalyzed by protein farnesyltransferase (FT)[1] (3), which is comprised of two heterologous α- (FTα) and β- (FTβ) subunits, is a major post-translational lipid modification, together with protein geranylgeranylation (3). FT and protein geranylgeranyltransferase type I (GGT-I) catalyze the transfer of the farnesyl and geranylgeranyl group from farnesyl pyrophosphate (FPP) and geranylgeranyl pyrophosphate, respectively, to the cysteine residue of a C-terminal C*aaX* of small GTPases including Ras, Rac, and Rho, where C is cysteine, *a* is usually an aliphatic amino acid, and *X* is any amino acid. Marked differences in substrate specificity have been shown between FT and GGT-I, *i.e.* FT mainly utilizes, as substrates, small GTPases possessing the terminal C*aaX* motif, when *X* is serine, methionine, glutamine, cysteine, or alanine (4), whereas GGT-I prefers proteins with the C-terminal C*aa*L or C*aa*F motif (4). Among well characterized Ras proteins that terminate with a C*aaX* motif, human H-Ras-CIMF, N-Ras-CVVM, K-RasA-CIIM, and Rap2-CNIQ are known to be farnesylated by FT, while Rap1A-CLLL, as well as Rho family proteins are geranylgeranylated by GGT-I. It has also been shown that K-RasB-CVIM can be either farnesylated by FT or geranylgeranylated by GGT-I (5). Since constitutively active mutations of Ras proteins have been shown to induce carcinogenesis (6–8), which is suppressed by the inhibition of farnesylation, FT has attracted attention as a target of cancer chemotherapy (9). In addition, several compounds targeting FT have proven promising against African sleeping sickness caused by *Trypanosoma brucei* and Malaria caused by *Plasmodia* species (10).

Entamoeba histolytica is an intestinal protozoan parasite, which causes amebic dysentery, colitis, and liver abscess in humans, and is responsible for an estimated 50 million cases of amebiasis and 40–100 thousand deaths annually (11). A number of small GTPases have been studied including Ras/Rap (12, 13), Rho/Rac (14–18), and Rab (19–21). The completion of the *E. histolytica* genome data base will help us to comprehensively understand the presence and complexity of these small

* This work was supported by a Grant for Precursory Research for Embryonic Science and Technology (PRESTO), Japan Science and Technology Agency (to T. N.), a Health Sciences Research Grant for Research on Emerging and Re-emerging Infectious Diseases from Ministry of Health, Labour, and Welfare (to A. M. and T. N.), Grants-in-aid for Scientific Research from the Ministry of Education, Culture, Sports, Science and Technology of Japan (to A. M., 13670256 and to T. N., 15019120, 15590378), and a grant for the Project to Promote Development of Anti-AIDS Pharmaceuticals from Japan Health Sciences Foundation (to T. N). The costs of publication of this article were defrayed in part by the payment of page charges. This article must therefore be hereby marked "*advertisement*" in accordance with 18 U.S.C. Section 1734 solely to indicate this fact.

The nucleotide sequence(s) reported in this paper has been submitted to the GenBank™/EBI Data Bank with accession number(s) AB083372 (FTα of *E. histolytica*), AB083373 (FTβ of *E. histolytica*), AB112425 (*Eh*Ras3), and AB112426 (*Eh*Ras4).

** To whom correspondence should be addressed: Dept. of Parasitology, National Institute of Infectious Diseases, 1-23-1 Toyama, Shinjuku-ku, Tokyo 162-8640, Japan. Tel.: 81-3-5285-1111 (ext. 2733); Fax: 81-3-5285-1173; E-mail: nozaki@nih.go.jp.

[1] The abbreviations used are: FT, protein farnesyltransferase; GGT-I, protein geranylgeranyltrasferase type I; FTα, α-subunit of farnesyltransferase; FTβ, β-subunit of protein farnesyltransferase; *Eh*FT, farnesyltransferase of *E. histolytica*; FPP, farnesyl pyrophosphate; NTA, nitrilotriacetic acid; GTPγS, guanosine 5′-3-*O*-(thio)triphosphate, NJ, neighbor-joining.

GTPases in the ameba. The molecular and cellular functions of some of these small GTPases have begun to be unveiled (12, 17, 18, 22). However, the molecular basis of the lipid modification of these small GTPases remains largely unknown in this parasite.

In this report, we describe the molecular and biochemical characterization of the α- and β- subunits of FT of *E. histolytica* (*Eh*FT) using recombinant proteins co-expressed in *Escherichia coli*. We also show that only one amebic Ras protein among the many small GTPases tested is farnesylated by *Eh*FT. In addition, we show that the amebic FT exhibits marked resistance to a variety of compounds that are known to inhibit mammalian FT, indicating that the amebic FT possesses distinct biochemical properties from the mammalian FT.

EXPERIMENTAL PROCEDURES

Parasite—Trophozoites of *E. histolytica* strain HM-1:IMSS cl6 (23) were cultured axenically in BI-S-33 medium at 35.5 °C (24).

Chemicals—Recombinant human H-Ras-CVLS (wild type), H-Ras-CVLL (mutant type), FPT inhibitor-I {(*E,E*)-2-[(dihydroxyphosphinyl)-methyl]-3-oxo-3-[(3,7,11-trimethyl-2,6,10-dodecatrienyl)-amino]propanic acid, trisodium salt}, FPT inhibitor-II {(*E,E*)-2-[2-oxo-2-[[(3,7,11-trimethyl-2,6,10-dodecatrienyl)oxy]amino]ethyl]phosphonic acid, disodium salt}, Gliotoxin, α-hydroxyl farnesylphosphonic acid, and a peptidomimetic inhibitor FTI-276 {*N*-[2-phenyl-4-*N*-[2(R)-amino-3-mercaptopropylamino]benzoyl]-methionine]} were obtained from EMD Biosciences (San Diego, CA). [^{3}H]FPP (16.1 Ci/mmol) and [^{3}H]geranylgeranyl pyrophosphate (23.0 Ci/mmol) were purchased from PerkinElmer Life Sciences (Boston, MA), and [^{35}S]GTPγS (1,173 Ci/mmol) was obtained from Amersham Biosciences (Piscataway, NJ). Restriction endonucleases and modifying enzymes were purchased from Takara Biochemical (Tokyo, Japan). The other chemicals and reagents used were from either Sigma-Aldrich Fine Chemicals (Tokyo, Japan) or Wako Pure Chemical Industries (Osaka, Japan) unless otherwise mentioned and of the highest purity available.

cDNA Library of E. histolytica—A trophozoite cDNA library of *E. histolytica* was constructed using the poly(A)$^+$ RNA and λZAP II phage (Stratagene, La Jolla, CA) as described previously (25).

Identification and Cloning of FTα and FTβ of E. histolytica—We designed oligonucleotide primers to amplify FTα and FTβ protein-coding regions from *E. histolytica* by PCR based on a homology search using yeast and mammalian FT in the *E. histolytica* genome data base available at The Institute for Genomic Research (www.tigr.org/tdb/). The sense primer for *EhFTα* was 5′-ATGGAAGAAGACGAAGAAATCACATTTG-3′. Sense and antisense primers for *EhFTβ* were 5′-ATGGAAATTGAAGAAGTAGAAGTAGAAACTGTTAC-3′ and 5′-TTAGAGCGAACGGAAATACTCACAACGCTTATC-3′, respectively. Since we did not find a sequence containing the C terminus of FTα in the data base, we used T7 primer, located downstream of the cloning site of our cDNA library, to amplify the FTα-coding region. PCR was performed using a one-hundredth volume of the cDNA phage lysate as template with the following parameters. An initial step of denaturation at 94 °C for 3 min was followed by 30 cycles of denaturation at 94 °C for 1 min, annealing at 55 °C for 2 min, and extension at 72 °C for 2 min. A final step at 72 °C for 10 min was used to complete the extension. The amplified DNA fragments were electrophoresed, purified using a Geneclean II kit (BIO101, La Jolla, CA), and cloned into the SmaI site of pUC18 using a SureClone Ligation Kit (Amersham Biosciences). Nucleotide sequences were confirmed with an ABI Prism BigDye terminator cycle sequencing ready reaction kit (PE Applied Biosystems, Foster City, CA) on an ABI Prism 310 Genetic Analyzer.

Identification and Cloning of Ras Small G Proteins of E. histolytica—To identify substrates for the amebic FT, we searched for putative Ras homologues in the *E. histolytica* Genome data base via a TBLASTN search using amebic (*Eh*Ras1and *Eh*Ras2) and mammalian Ras as inquiry sequences. We identified 8 previously uncharacterized putative full-length Ras genes. The C terminus of these Ras proteins ended with Phe (four genes), Leu (two), Met (one), or Ala (one). The two latter genes encoding putative Ras proteins containing the CSVM- or CVVA-C terminus (identical to EH02830 and EH01021 in the *E. histolytica* genome data base) were assumed to be good candidates to be farnesylated by the amebic FT, designated *Eh*Ras3 and *Eh*Ras4, respectively, and characterized further. A protein coding region of *Eh*Ras1-4, and *Eh*RacC were amplified by PCR using cDNA as template and appropriate primers based on the sequences in the genome data base.

Sequence Analysis—FTα and FTβ protein sequences from *E. histolytica* and 9 other organisms, and 20 putative Ras and Ras-related proteins of *E. histolytica* were retrieved from the TIGR and the National Center for Biotechnology Information data bases (www.ncbi.nih.gov/) using the BLASTP and TBLASTN algorithms. The protein alignment and phylogenetic analyses were performed with ClustalW version 1.81 (26) using the neighbor-joining (NJ) method (27) with the Blosum matrix created using the ClustalW program (26). Unrooted NJ trees were drawn with TreeView ver.1.6.0 (28). Branch lengths and bootstrap values (1000 replicates) (29) were derived from the NJ analysis.

Construction of a Plasmid to Express Recombinant EhFT—A plasmid containing the protein-coding regions of FTα (without the stop codon), FTβ (with the stop codon), and the ribosome binding sequence (GAGGAGTTTTAACTT) between them were constructed by three rounds of PCR using the recombinant approach (30, 31). Briefly, two sets of initial PCRs were conducted to amplify the FTα and FTβ protein-coding region using a sense primer, 5′-ATGGAAGAAGACGAAGAAATCACATTTG-3′ and an antisense primer, 5′-ATGATTAGTAATTTTTGTTAAATACCAATCCC-3′ (for FTα); a sense primer, 5′-ATGGAAATTGAAGAAGTAGAAGTAGAAACTGTTAC-3′ and an antisense primer, 5′-TAAGAGCGAACGGAAATACTCACAAGCCTTATC-3′ (for FTβ). Two sets of second PCRs were conducted using the respective product of the first reaction as a template. To amplify the FTα protein-coding region (excluding the stop codon), flanked by a BamHI site (italicized) and the ribosome binding site (underlined), a sense primer, 5′-GG*AGGATCC*CATGGAAGAAGACGAAGAAATCACATTTG-3′ (primer 1) and an antisense primer, 5′-AAGTTAAAACTCCTCATGATTAGTAATTTTTGTTAAATACCAATCCC-3′, were used. To amplify the FTβ sequence including the stop codon, flanked by the ribosome binding site (underlined) and a HindIII site (italicized), sense, 5′-GAGGAGTTTTAACTTATGGAAATTGAAGAAGTAGAAGTAGAAACTGTTAC-3′ and antisense, 5′-CCA*AGCTT*TAAGAGCGAACGGAAATACTCACAAGCCTTATC-3′ (primer 2) were used. The third round of PCR was conduced using a mixture of the products of the second round, and primers 1 and 2. The resulting 2.1-kb PCR product was digested with BamHI and HindIII and ligated into BamHI- and HindIII-double digested pQE31 to construct pEhFTαβ. In pEhFTαβ, the FTα and FTβ protein-coding regions placed in tandem were presumably translationally coupled, facilitating co-expression of these two subunits at similar levels. An N-terminal histidine tag was also engineered in EhFTα to facilitate purification.

Construction of Plasmids to Express Recombinant Small GTPases—A protein-coding region of *Eh*Ras1-4, and *Eh*RacC flanked by additional BamHI and SalI sites (italicized), were amplified by PCR using cDNA as a template and sense and antisense primers: 5′-GGA*GAATCC*CATGACTGCCAATACATATAAATTAGTTATG-3′ and 5′-CC*AGTCGAC*TTAGAACATTATGCATTTCTTTTCTTTCTT-3′ (*Eh*Ras1); 5′-GGA*GAATCC*CATGACTACAAATACTTATAAATTAGTTATGCTTG-3′ and 5′-CCA*GTCGAC*TTATAACAATTCACACTTTGATTTAGAAGG-3′ (*Eh*Ras2); 5′-GGA*GAATCC*CATGAGTTTAAAAAGAATTGTTATGCTTGGA and 5′-CCA*GTCGAC*TTACATAACAGAACATCCAATTTTCTTATA-3′ (*Eh*Ras3); 5′-GGA*GAATCC*CATGAACTCAACAATAAAAAGAATATCTGTT-3′ and 5′-CCA*GTCGAC*TTAAGCAACCACACATGAAGTATTATTCTC-3′ (*Eh*Ras4); 5′-GGA*GAATCC*CATGAGTGAAAAACCCACATCAAT-3′ and 5′-CCA*GTCGAC*TTATAAAAGAGCACACTTTGACCTTTG-3′ (*Eh*RacC), where restriction sites are italicized. PCR products were electrophoresed, purified, and cloned into BamHI- and SalI double-digested pQE31 plasmid to obtain pEhRas1-4 and pEhRacC. The resulting plasmids were designed to contain an N-terminal histidine tag to facilitate purification. Plasmids to express an N-terminal Nus fusion protein of *Eh*Rap2 and a glutathione S-transferase-*Eh*Rab5 or glutathione *S*-transferase-*Eh*Rab7 fusion protein were constructed using pET-43.1a and pGEX4T-1 with appropriate restriction sites included in PCR primers. The characterization of *Eh*Rab5, *Eh*Rab7, and *Eh*Rap2 and details of the construction of these expression plasmids are described elsewhere.

Expression and Purification of Recombinant Proteins—Plasmids constructed as described above were introduced into *E. coli* M15 cells. A 12-ml seed culture was grown overnight at 37 °C in LB medium containing 100 μg/ml of ampicillin and 25 μg/ml of kanamycin. The overnight culture was then inoculated into 250 ml of fresh medium containing the antibiotics. The bacteria were grown for 1 h, and then another 4 h after the addition of 1 mM isopropyl-1-thio-β-D-galactopyranoside to induce protein expression. The bacteria were harvested by centrifugation at 4,000 × *g* for 20 min, and the pellet was stored at −20 °C until purification. The recombinant proteins were purified according to the manufacturer's instructions. Briefly, the bacterial cells were resus-

pended in cold lysis buffer, phosphate-buffered saline, pH 8.0, containing 10 mM imidazole and 1% lysozyme, sonicated, and centrifuged at 10,000 × *g* for 20 min. The supernatant was applied to a Ni-NTA-agarose column (Qiagen, Hilden, Germany), washed extensively with the wash buffer containing 20 mM imidazole, and eluted with the lysis buffer containing 250 mM imidazole. The recombinant FT proteins were further purified with Q Sepharose Fast Flow (Amersham Biosciences) at a flow rate of 0.5 ml/min as described (32). The purified recombinant FT and Ras proteins were then dialyzed against the enzyme assay buffer described below and 40 mM Tris-HCl, pH 8, containing 90 mM NaCl, 10 mM $MgCl_2$, and 2 mM dithiothreitol and stored with 20 and 50% glycerol, respectively, at −80 °C until use. Protein concentrations were determined by the method of Bradford (33) using Protein Assay CBB solution (Nacalai Tesque, Kyoto, Japan). Bovine serum albumin was used as the protein standard.

Protein Analyses—The expression and purity of recombinant proteins were evaluated by standard SDS-PAGE as described (34). To prepare *E. histolytica* extracts, trophozoites were washed three times with ice-cold phosphate-buffered saline, resuspended at 10^7/ml in phosphate-buffered saline containing a proteinase inhibitor mixture (1 mM phenylmethylsulfonyl fluoride, 1 nM trypsin inhibitor, 100 μM *trans*-epoxysuccinyl-L-leucylamino-(4-guanidino)butane, 1 μg/ml pepstatin A, 1 μg/ml leupeptin, 1 μg/ml *N*-α-p-tosyl-L-lysine chloromethyl ketone hydrochloride, and 1 mM benzamidine hydrochloride), and subjected to 3 cycles of freezing and thawing. After centrifugation at 10,000 × *g* for 10 min, the supernatant was subjected to further analyses.

Enzyme Assays—The enzymatic activity of recombinant FT and the whole lysate of *E. histolytica* trophozoites were assayed for incorporation of [^{3}H]farnesyl pyrophosphate or [^{3}H]geranylgeranyl pyrophosphate into the recombinant small GTPases prepared as described above, human H-Ras-CVLS, or H-Ras-CVLL. The assay was performed essentially as described previously (35) with minor modifications. Briefly, in standard assays, the reaction mixture contained, in a total volume of 50 μl, 50 mM HEPES (pH 7.5), 5 mM $MgCl_2$, 20 μM $ZnCl_2$, 5 mM dithiothreitol, 0.1% polyethylene glycol 20,000, 187 nM [^{3}H]FPP (3 μCi/ml), or [^{3}H]geranylgeranyl pyrophosphate (3 μCi/ml), and 240 to 750 μM of the purified recombinant FT or 1.9 mg/ml of the *E. histolytica* lysate. The reaction was initiated by the addition of either the recombinant enzyme or cell extracts, run at 30 °C for 20 min, and terminated by the addition of 200 μl of 10% HCl in ethanol. The quenched reactions were allowed to stand at room temperature for 15 min. After the addition of 200 μl of 100% ethanol, the reactions were vacuum-filtered through glass filter GF/C (Whatman, Maidstone, UK) using a Sampling Manifold (Millipore Corp., Bedford, MA). The filters were washed with 4 ml of 100% ethanol and then subjected to scintillation counting (LS 6,000IC, Beckman Coulter, Fullerton, CA). The K_m value was calculated from Lineweaver-Burk plots. FT assays were also conducted in the presence of known FT inhibitors: farnesylpyrophosphate analogues (FPT inhibitor-I, FPT inhibitor-II, Gliotoxin, α-hydroxyl farnesylphosphonic acid) and a peptidomimetic inhibitor (FTI-276) under the condition described above.

Guanine Nucleotide Binding Assays—GTP binding activity was measured using [^{35}S]GTPγS (Amersham Biosciences) and a nitrocellulose filter (Millipore HA filter, Millipore Corporation) as previously described (36).

RESULTS

Features of FTα and FTβ of E. histolytica—Nucleotide sequences of *Eh*FTα and *Eh*FTβ obtained by PCR were identical to sequences available from the genome data base (EH02829 and EH04188, respectively). The putative protein-coding region of *Eh*FTα and *Eh*FTβ, consisting of 894 and 1,125 bps, encodes proteins of 298 and 375 amino acids with a calculated molecular mass of 35.6 and 42.6 kDa and a pI of 5.4 and 5.7, respectively. A search for previously identified domains and motifs (37) using the NCBI Conserved Domain Search revealed that both *Eh*FTα and *Eh*FTβ contained well conserved signature domains shared by other organisms. *Eh*FTα contained one BET4 domain and five "protein prenyltransferase α-subunit repeats"; *Eh*FTβ possessed one CAL1 domain and five "prenyltransferase and squalene oxidase repeats" (Fig. 1). The deduced protein sequences of *Eh*FTα and *Eh*FTβ were aligned with those from other organisms using the ClustalW program (Fig. 1). Both *Eh*FTα and *Eh*FTβ were the smallest in size, and lack any recognizable secretory signal sequence, an organelle targeting signal, and any domain implicated in membrane association including the transmembrane domain and myristylation signal. *Eh*FTα and *Eh*FTβ also lack the N-terminal extension of 15–58 amino acids found in these subunits from other organisms. *Eh*FTα showed 29, 30, 27, and 24% positional identity with FTα of human, *Arabidopsis thaliana, Saccharomyces cerevisiae*, and *T. brucei*, respectively; *Eh*FTβ revealed 36, 35, 28, and 31% positional identity with the FTβ of these organisms, respectively. All the residues implicated to be essential for catalysis (Fig. 1, *A* and *B*) (39–41) are conserved in both *Eh*FTα and *Eh*FTβ.

Phylogenetic Analysis of EhFTα and FTβ—Phylogenetic trees of *Eh*FTα and *Eh*FTβ were constructed (Fig. 2). Neither the α- nor β-subunit of the amebic FT showed statistically significant (*i.e.* supported with high bootstrap values) affinity to those from other organisms while trypanosomal, mammalian, and plant proteins encoding α- and β-subunits formed well supported independent clades, representing distinct groups. These results were compatible with the notion that both subunits of *Eh*FT developed independently from other eukaryotes, suggestive of the presence of unique biochemical properties of *Eh*FT (see below).

Expression of EhFT in E. coli—A complex consisting of *Eh*FTα and *Eh*FTβ was expressed and purified as described under "Experimental Procedures." Purified proteins revealed two major proteins with an equal intensity of an apparent molecular mass of 38 and 43 kDa (Fig. 3), which likely correspond to *Eh*FTα and *Eh*FTβ, respectively. The apparent molecular mass of α- and β-subunits agreed well with a theoretical value of 37.6 kDa with the N- and C-terminal addition of MRGSHHHHHHTDP and EEF, respectively, for the recombinant *Eh*FTα and 42.6 kDa for *Eh*FTβ. When histidine-tagged *Eh*FTα or *Eh*FTβ were expressed separately, the apparent molecular mass of these proteins agreed well with their identity (data not shown). Densitometric quantitation of these two bands also supported that they contain an equal number of protein molecules (data not shown). Gel filtration chromatography of the recombinant *Eh*FT using Sephacryl S-300 revealed a molecular mass of about 80 kDa (data not shown). Thus, the recombinant *Eh*FTα and *Eh*FTβ were present as a stable dimer during the process of purification by Ni-NTA agarose and Q Sepharose Fast Flow chromatography (Fig. 3). After the purification, recombinant *Eh*FT was estimated to be >95% pure by densitometric quantitation (data not shown), and further utilized for enzymatic assays.

Demonstration of FT Activity of the Recombinant EhFT against Human Ras Proteins—When assayed for incorporation of [^{3}H]farnesyl pyrophosphate, the recombinant *Eh*FT showed FT activity [1.03 ± 0.012 nmol of FPP/mg of protein (mean ± S.E.)] against human recombinant wild-type H-Ras-CVLS, whereas it showed ~20-fold less activity against mutant H-Ras-CVLL (0.05 ± 0.01 nmol of FPP/mg of protein) (Fig. 4), which was previously shown to be predominantly geranylgeranylated by human GGT-I. The addition of EDTA (10 mM) to the reaction mixtures completely abolished the enzymatic activity of the recombinant *Eh*FT (data not shown), suggesting, as shown for mammalian and yeast FT, that *Eh*FT also requires Zn^{2+} and Mg^{2+} for its activity.

Identification and Phylogenetic Analysis of the Novel Ras Proteins in E. histolytica—To identify the protein substrates of *Eh*FT in the parasite, we searched for putative Ras proteins in the genome data base based on homology to the *Eh*Ras1 and human H-Ras. In addition to *Eh*Ras1, *Eh*Ras2, *Eh*Rap1, and *Eh*Rap2, which have already been reported (12), we found 8 additional putative ras proteins previously uncharacterized, with the C-terminal C*aaX* motif. Of these 8 proteins, 6 possess

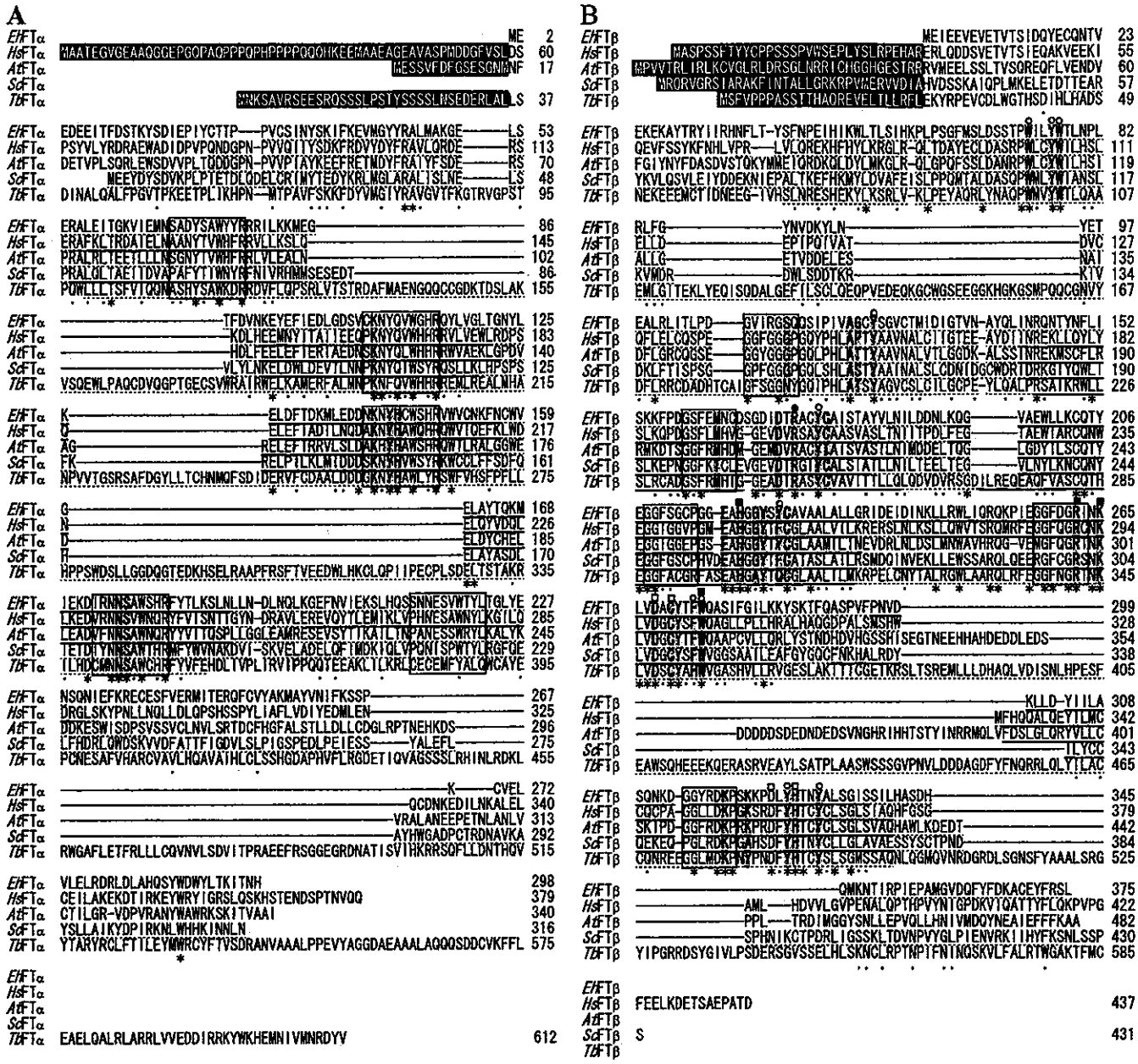

FIG. 1. **Alignment of the deduced amino acid sequences of α- (*A*) and β- (*B*) subunits of protein farnesyltransferase of *E. histolytica* with those from other organisms.** *Eh*, *Entamoeba histolytica*; *Hs*, *Homo sapiens*; *At*, *A. thaliana*; *Sc*, *S. cerevisiae*; *Tb*, *T. brucei*. *Asterisks* (*) under the alignments indicate identical amino acid residues and *dots* (.) indicate conserved amino acid substitutions. BET4 (in *A*) and CAL1 (in *B*) domains detected by the NCBI Conserved Domain Search are *dotted-underlined* (partially *solid underlined*). The prenyltransferase α-subunit repeats and the prenyltransferase/squalene oxidase repeats, also detected by the search, are indicated by *solid underline* in *A* and *B*, respectively. The regions corresponding to the motif *P*XNY*XX*WYR (37), previously found in the turns connecting two helices of the coiled-coil, in FTα and a glycine-rich motif GG*F*X*G*X*X*P (37), corresponding to the loop regions that connect the C termini of the peripheral helices with the N termini of the core helices in the barrel (38) in FTβ are *boxed*. All amino acids implicated in catalysis by crystallographic and mutational studies of mammalian FTs (38–41) are shaded. Aromatic amino acids located in the hydrophobic cleft at the center of the α-α barrel implicated in the interaction with the farnesyl residue are marked with *open circles* (38). Arg^{202} implicated in the binding of the essential C-terminal carboxylate of the protein substrate is marked with a *filled circle* (39). Amino acids implicated in the coordination of zinc are marked with *open squares* (40). Amino acids implicated in the binding and utilization of FPP, shown by a mutational analysis (39) are marked with *filled squares*. N-terminal extensions absent in *Eh*FTα and *Eh*FTβ are also *boxed*. DDBJ/EMBL/GenBank™ accession numbers are given in Fig. 2.

Phe or Leu (4 with Phe, 2 with Leu) at the C terminus, while 1 each has Met or Ala. We tentatively designated proteins possessing Met or Ala as *Eh*Ras3 or *Eh*Ras4, and the other proteins as *Eh*Ras5–10. The nucleotide sequence of the *Eh*Ras1 cDNA we cloned was identical to that previously reported; the nucleotide sequence of our *Eh*Ras2 cDNA differed at one nucleotide (A368G) from the sequence previously reported (12), resulting in a Y123C substitution. *Eh*Ras3 and 4 consisted of 210 and 182 amino acids with a calculated molecular mass of 23.9 and 20.6 kDa and a pI of 5.5 and 5.8, respectively. The ClustalW multiple alignment showed that *Eh*Ras3 and 4, together with the previously identified *Eh*Ras1, *Eh*Ras2, *Eh*Rap1, and *Eh*Rap2, share conserved GTP binding consensus sequences (42) and also, at a moderate level, the effector binding region (42) (Fig. 5*A*).

Percent identity among the *Eh*Ras1-4 and *Eh*Rap1-2 (Fig. 5*B*) also indicates that *Eh*Ras3 is, together with *Eh*Ras5 and *Eh*Ras6 (*Eh*Ras5 *versus* *Eh*Ras1-2, 62–66%; *Eh*Ras6 *versus* *Eh*Ras1-2, 39–41%; *Eh*Ras5 and *Eh*Ras6 were not studied further in the present work) closely associated with *Eh*Ras1

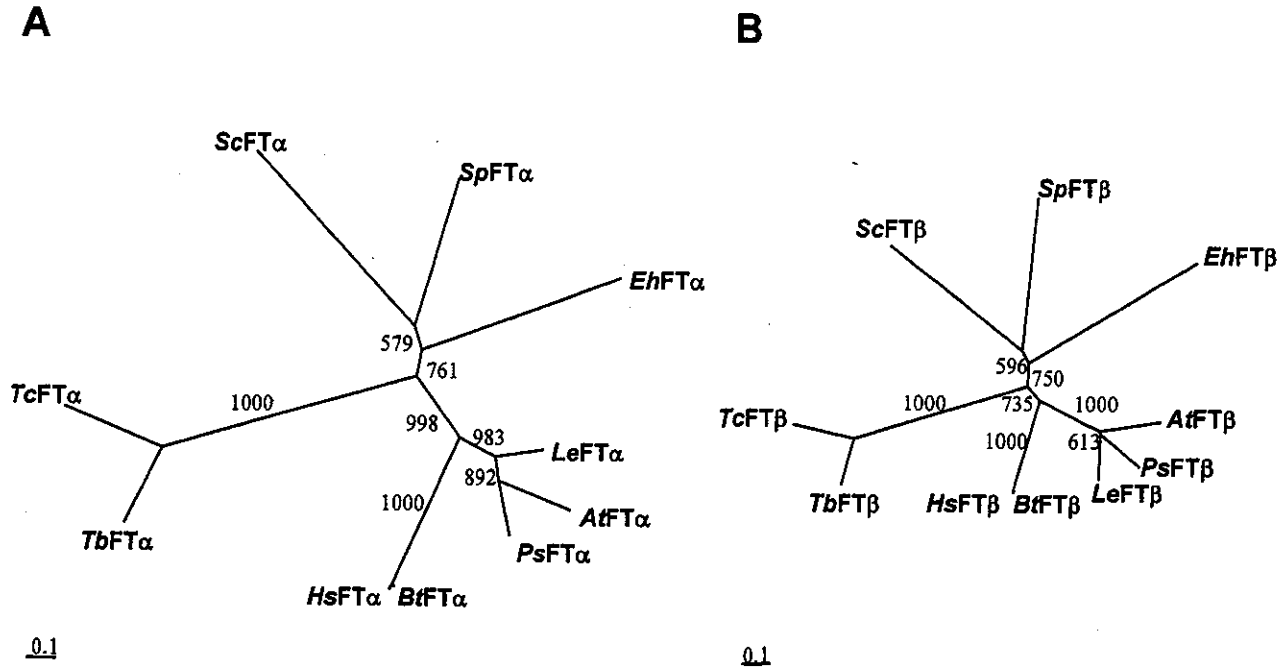

FIG. 2. **Phylogenetic trees of FTα (*A*) and FTβ (*B*).** Only FTα and FTβ protein sequences that were previously characterized enzymologically were included. The *trees* were constructed by Neighbor-joining distance analysis using the ClustalW and TreeView programs. *Line lengths* indicate distances between nodes. The *bar* represents a distance of 0.1 amino acid changes per site. Bootstrap values for 1,000 replicates are shown at nodes. Abbreviations are: *Eh*, *E. histolytica* (DDBJ/EMBL/GenBank™ number of FTα and FTβ, AB083372, AB083373); *Sc*, *S. cerevisiae* (P29703, P22007); *Sp*, *Schizosaccharomyces pombe* (O60052, O13782); *Tb*, *T. brucei* (AAF73919, AAF73920); *Tc*, *T. cruzi* (AAL69904, AAL69905); *At*, *A. thaliana* (Q9LX33, AAF74564); *Ps*, *Pisum sativum* (O24304, Q04903); *Le*, *Lycopersicon esculentum* (P93277, AAC49666); *Bt*, *Bos taurus* (NP_803464, P49355). *Hs*, *Homo sapiens* (NP_002018, NP_002019).

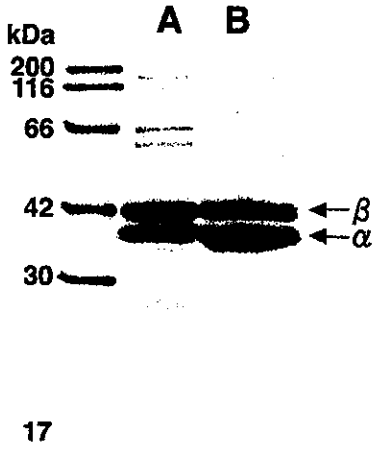

FIG. 3. **SDS-PAGE analysis of the purified recombinant FT of *E. histolytica*.** Both *Eh*FT subunits were coexpressed in *E. coli*, copurified on Ni-NTA agarose (*lane A*), or further purified with anion exchange Q Sepharose Fast Flow (*lane B*). Samples were subjected to SDS-PAGE and stained with Coomassie Brilliant Blue.

and *Eh*Ras2, showing 48–51% identities, whereas *Eh*Ras4 showed only 26–30% identities to *Eh*Ras1, *Eh*Ras2, *Eh*Rap1, and *Eh*Rap2. Phylogenetic reconstructions (Fig. 6) confirmed the results of the protein alignment: both *Eh*Ras3 and *Eh*Ras4, together with *Eh*Ras5 and *Eh*Ras6, represent new members of the Ras/Rap family. Rac and Rab proteins were categorized to independent clades, whose association was well supported by moderate to high bootstrap values (only representative Rac and Rab proteins were included in this analysis).

Identification of EhRas4 as a Substrate of Eh FT—We tested substrate specificity of *Eh*FT toward *Eh*Ras1-4. We chose *Eh*Ras3-4, together with *Eh*Ras1-2, as possible candidates for *Eh*FT substrates because it was previously shown that mammalian and yeast small GTPases with a C-terminal Ser, Met, Gln, Cys, or Ala have a tendency to be farnesylated whereas those containing Phe or Leu at the C-terminal end tend to be geranylgeranylated (4). The recombinant *Eh*FT showed farnesyltransferase activity toward *Eh*Ras4 (1.03 ± 0.005 nmol of FPP/mg of protein), which was comparable to the activity toward human H-Ras-CVLS (Fig. 4). In contrast, *Eh*FT showed no detectable or only minimal activity toward *Eh*Ras1-3. We also tested if *Eh*Rab, *Eh*Rac, or *Eh*Rap are farnesylated by *Eh*FT. The recombinant *Eh*FT did not transfer farnesyl to *Eh*Rab7, *Eh*RacC, or *Eh*Rap2 (data not shown). Furthermore, the recombinant *Eh*FT did not utilize geranylgeranyl pyrophosphate as a isoprenyl donor to transfer the geranylgeranyl residue to *Eh*Ras1, *Eh*Ras2, *Eh*Ras3, *Eh*Ras4, *Eh*Rap2, *Eh*RacC, or *Eh*Rab7 (data not shown). To confirm that *Eh*Ras3 and 4 are capable of binding GTP, a GTP binding assay was conducted. Both *Eh*Ras3 and 4 showed comparable GTP-binding activity to *Eh*Ras2 and *Eh*Rab7 (data not shown). We also assayed for the FT activity in the whole lysate of the *E. histolytica* trophozoites. Among the 2 human H-Ras and 4 *E. histolytica* Ras homologues described above, FT activity was detected only against human H-Ras-CVLS and *Eh*Ras4 in the whole lysate (data not shown), which excluded the possibility that some other *Eh*FT protein (or proteins) exists to farnesylate these small GTPase in the amebic lysate.

Kinetic Properties of EhFT—Lineweaver-Burk plots showed the K_m of recombinant *Eh*FT for *Eh*Ras4 to be 5.13 ± 0.02 μM (plots not shown), significantly higher than that of bovine FT, the K_m of which for Ras-CVLS and Ras-CVIM is 0.63 ± 0.05

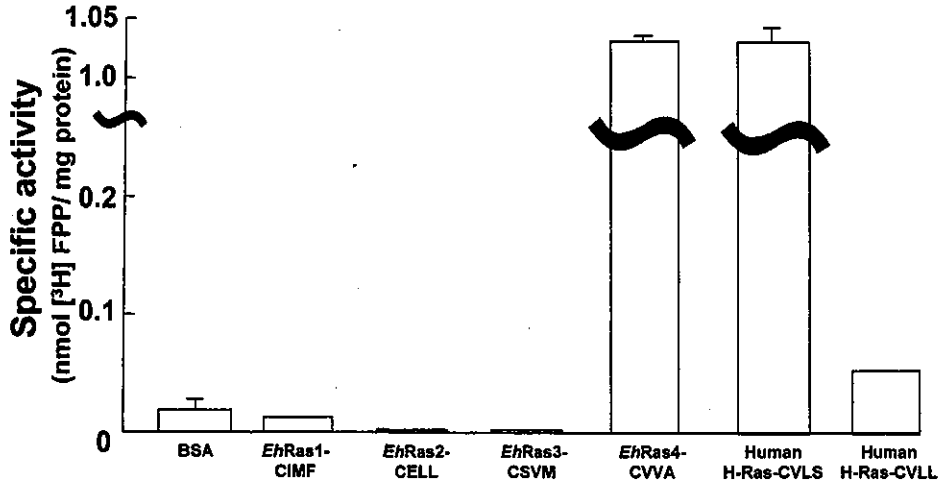

FIG. 4. **Substrate specificity of recombinant FT of *E. histolytica*.** The specific activity of the recombinant *Eh*FT was determined from the incorporation of [^{3}H]farnesyl pyrophosphate into the recombinant *Eh*Ras1, human wild type H-Ras-CVLS, and mutant type H-Ras-CVLL. Means ± S.E. of quadruplicates are shown.

A

```
                    GXXXXGKS                DXT
EhRas1    MTANTYKLVMLGGGAVGKSAITVQLVSGHFVQIYDPTIEDSYRTSISVDGEMVSLDIL  58
EhRas2    MTTNTYKLVMLGGGAVGKSAITVQLVSGHFVQIYDPTIEDSYRTSISVDGEMVSLDIL  58
EhRas3      MSLKRIVMLGTGAVGKSAITLQYVSHYFASDYNPTIEDSFRTSITIGDDNYPIEIL  56
EhRas4  MNSTIKRISVVLLGDHGVGKSSVAIRFATNVFMSEYSIHPKQIQVSRVSVDGTDYDIGVI  60
EhRap1    MPVKDYKIVVLGSGADGKSSITVRFVQGIFLVKYDPTIEDSYRKQLDLDGQQYVLEIL  58
EhRap2    MPVKDYKIVVLGSGAVGKSSITVRFVQGIFLVKYDPTIEDSYRKQLDLDGQQYVLEIL  58
                DXAG
EhRas1  DTAGQEEYSALRDQYMRSGDGYVIVYSITSTTSFLEANGFREQLYRVLDKDVSEHVSIAL 118
EhRas2  DTAGQEEYSALRDQYMRSGDGYVIVYSITSTTSFLEANGFREQLYRVLDKDVSEHVSIAL 118
EhRas3  DTAGQEEFDALKDTYIRSGDGFAIVYSITSLNTFLEANEIRERIYRVLDKDPSQHIPICL 116
EhRas4  DTN—ATMTIQNDDLIMKGDAFVVMYSVTNKNSFLHLPLYLNRIYELRK-DHSKTIPIII 117
EhRap1  DTAGTEQFTAMRDLYMKTGQGFVLVYSIIAQSTYNDLDPIHDQIVRVRD——TEDVPIIV 115
EhRap2  DTAGTEQFTAMRDLYMKTGQGFVLVYSIMAQSTYNDLDPIHDQIVRVRD——TENVPIIV 115
                NKXD                EXSAX
EhRas1  CGNKCDLESEROVQTNEAKNLAEQWKVLFFETSAKAKINITETFQALVKDIKANRAATEP 178
EhRas2  CGNKYDLENERQVETAEAKKLADEWKVLFFETSAKAKINITETFQALVKDIKVNRVSSEP 178
EhRas3  VGNKSDLESERIVSKEQAEELAGLWGISFIETSAKKKSNINELYQIIMKDIIDTKTKEDE 176
EhRas4  VGNKCDEK-RREVIYESGQLFSDSISCLFMETSALDYTNINHLFDIIIREWVSFHPVENN 176
EhRap1  VGNKCDLESQRIVSQDDGKALADKYGADFLEVSAKAEIRISDIFTTLIKRINSSNGNKKP 175
EhRap2  VGNKCDLESQRIVSQDDGKALADKYGAEFLEVSAKAEIRISDIFTTLIKRINAMNQTKPK 175

EhRas1  SATTAEANDSKGKKDKKEKKEKKCIMF                                  205
EhRas2  -TASIEPTDTKGKKERKPSKSKCELL                                   203
EhRas3  EKKRLEEHESITKKSSKKQRDGKKFYKKIGCSVM                          210
EhRas4  ————T————SCVVA                                              182
EhRap1  ————D————HAHHCSLL                                           184
EhRap2  ————K————KSGGCSLF                                           184
```

B

	*Eh*Ras1	*Eh*Ras2	*Eh*Ras3	*Eh*Ras4	*Eh*Rap1	*Eh*Rap2
*Eh*Ras1		86	51	26	44	47
*Eh*Ras2			48	26	43	44
*Eh*Ras3				30	38	39
*Eh*Ras4					26	26
*Eh*Rap1						91
*Eh*Rap2						

FIG. 5. **Similarity among *Eh*Ras1-4 and *Eh*Rap1-2.** *A*, sequence alignment of *Eh*Ras1-4 and *Eh*Rap1-2 using the ClustalW program. Sequences over the alignment are GTP binding consensus sequences. *Asterisks* (*) and *dots* (.) indicate identical amino acids and conserved amino acid substitutions, respectively. G*XXXX*GKS and DXT depict G*XXXX*GK(S/T) and D(*X*)$_n$T consensus sequences, respectively. DDBJ/EMBL/GenBank™ accession numbers are given in Fig. 6. *B*, percentage identities among *Eh*Ras1-4 and *Eh*Rap1-2.

and 0.13 ± 0.03 μM, respectively (35).

Sensitivity of Recombinant EhFT to Human FT Inhibitors—We examined the sensitivity of *Eh*FT to known FT inhibitors. As shown in Table I, *Eh*FT was virtually insensitive at up to 30 μM except to FPT inhibitor-II and FPT 276 when recombinant *Eh*Ras4 was used as substrate. The lack of sensitivity of *Eh*FT

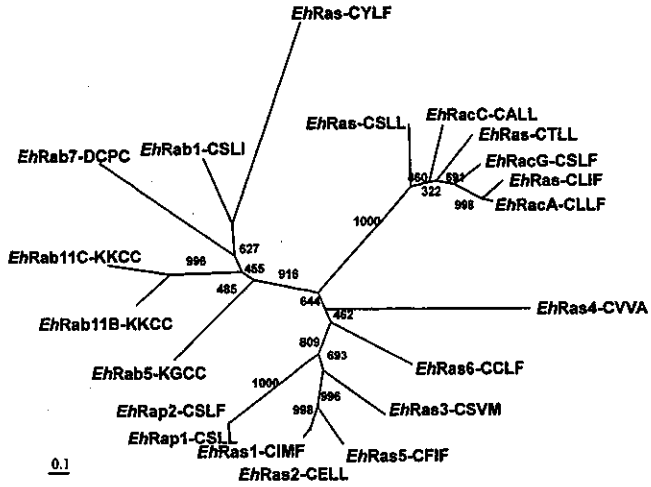

FIG. 6. **Phylogenetic tree of representative members of small GTPases of *E. histolytica* constructed by the Neighbor-joining method.** DDBJ/EMBL/GenBank™ accession numbers of these proteins are: *Eh*Ras1, AAA21446; *Eh*Ras2, AAA21447; *Eh*Ras3, AB112425; *Eh*Ras4, AB112426; *Eh*Rap1, AAA21444; *Eh*Rap2, AAA21445; *Eh*RacA, Q24814; *Eh*RacC, Q24816; *Eh*RacG, O76321; *Eh*Rab1, BAB40669; *Eh*Rab5, BAB40673; *Eh*Rab7, BAB40674; *Eh*Rab11b, BAB40678; *Eh*Rab11C, BAB40679. The other proteins without accession numbers shown in the tree are putative Ras superfamily small GTPases found in the *E. histolytica* genome data base. *Eh*Ras7-10 are labeled as *Eh*Ras-XXXX, because there is no sufficient evidence to support that these proteins are Ras homologues.

to FT inhibitors was not dependent on the substrate; *Eh*FT was also insensitive to these inhibitors when H-Ras-CVLS was used as a substrate.

DISCUSSION

In this study, we have demonstrated for the first time the molecular identity of FT in enteric parasitic protozoa. Although all major subgroups of small GTPases, *i.e.* Ras, Rap, Rho, Rac, Rab, Arf, and Ran, have been identified (12, 14–21) in *E. histolytica* and some of their functions studied (17, 18), this is the first demonstration and characterization of an isoprenylation enzyme essential for correct membrane topology and organelle targeting of these small GTPases. We identified common features of FT hitherto recognized in other eukaryotes: both FTα and FTβ contained well-conserved signature domains such as BET4 and CAL1 domains, and the repeats, *i.e.* protein prenyltransferase α-subunit repeats and prenyltransferase/squalene oxidase repeats (Fig. 1). *Eh*FT forms a heterodimeric

TABLE I
Inhibition of recombinant EhFT by inhibitors of human FT

The enzymic activity of recombinant *Eh*FT using *Eh*Ras4-CVVA and human H-Ras-CVLS as protein substrates was determined by incorporation of [^{3}H]FPP in the absence and presence of FT inhibitors to calculate IC_{50} values.

Inhibitors	IC_{50}		
	E. histolytica FT		Human FT[a]
	EhRas4	Human H-Ras	Human H-Ras
	μM		
Prenyl analogues			
FPT inhibitor-I	>30	>30	0.075[b]
FPT inhibitor-II	2.0	2.7	0.075[b]
Gliotoxin	>30	>30	1[c]
α-Hydroxyfarnesyl-phosphonic acid	>30	>30	0.03[d]
Peptidomimetic			
FTI-276	2.4	0.9	0.0005[e]

[a] Reported IC_{50} values of human FT for the inhibitors using human H-Ras-CVLS as a protein substrate are shown for comparison.
[b] Ref. 47.
[c] Ref. 48.
[d] Ref. 49.
[e] Ref. 50.

complex with a ratio of 1:1 between α- and β-subunits, similar to the case in other organisms, as shown by co-purification (Fig. 3). Phylogenetic analyses indicate that both *Eh*FTα and *Eh*FTβ are equally distant from homologues from other organisms. This may partially explain some of the unique biochemical characteristics of the amebic FT not shared by the mammalian counterpart. It is also worth noting that trees of both α- and β-subunits are similar (Fig. 2), suggesting that the FT subunits co-evolved independently at a comparable rate in these organisms.

We identified *Eh*Ras4-CVVA as one of the intrinsic substrates of FT in *E. histolytica*. Although it was not possible to test all small GTPases as substrates for *Eh*FT, we showed that *Eh*FT exclusively utilized *Eh*Ras4 as a farnesyl acceptor. In contrast, recombinant *Eh*Ras1-3, Rap2, RacC, and Rab7 were not farnesylated by recombinant *Eh*FT (Fig. 5) or the whole cell extract. The fact that the amebic lysate contained the activity to transfer the farnesyl residue to *Eh*Ras4, but not other *Eh*Ras isotypes, reinforces the notion that the FT characterized in the present study is the sole FT in this organism and also specific for this Ras protein. We also tentatively concluded that FT-mediated farnesylation is not a major lipidation of Ras protein in this organism. It was unexpected that *Eh*FT did not utilize *Eh*Ras3, which terminates with CSVM, as a farnesyl acceptor, because mammalian and yeast small GTPases containing a C-terminal Ser, Met, Gln, Cys, or Ala were shown to prefer to be farnesylated (4). An unexpected substrate specificity was also previously reported for FT from another protozoan parasite *T. brucei*, which farnesylates Ras protein with CVIM, but not CVLS (43). The fact that *Eh*FT prefers smaller amino acids at the C terminus of *Eh*Ras (CVV*A* and CVL*S*) indicates that the amebic FT may possess a smaller binding cleft for the Ras C terminus.

Among newly found putative Ras-like proteins, *Eh*Ras3–6 were the only ones that contained a terminal C*aaX* and also showed a closer kinship to *Eh*Ras1 and *Eh*Ras2 than to other small GTPases (*i.e.* Rap, Rac/Rho, and Rab) (Fig. 6). This observation, together with the lack of farnesylation by *Eh*FT of *Eh*Ras1–3, Rap2, RacC, and Rab7, indicates that *Eh*Ras4 protein is the sole Ras protein farnesylated by *Eh*FT. It is also conceivable that *Eh*Ras1–3 proteins with the C-terminal Phe, Leu, or Met, respectively, are farnesylated by GGT-I, as shown for rat RhoB-CKVL (44). This is also the case for *Eh*Ras2-CELL, which has been shown to be farnesylated by the recombinant *E. histolytica* GGT-I in our preliminary experiment (data not shown). Although the C terminus of the previously identified amebic Ras/Rap (*i.e.* *Eh*Ras1-2 and *Eh*Rap1-2) (12) was presumed to be geranylgeranylated, a study using rabbit reticulocytes lysates (as a source of enzyme) and recombinant *Eh*Ras1 and *Eh*Rap2 showed that these proteins were not geranylgeranylated, but farnesylated (13). Considering that recombinant *Eh*FT neither farnesylates nor geranylgeranylates *Eh*Ras1 and *Eh*Rap2, we have to conclude that the results of the previous report (13) are likely a consequence of artifactual farnesylation by heterologous prenylase(s), as observed for *Eh*Ras2-CELL, which was farnesylated by the rat GGT-I (data not shown). Alternatively, it is conceivable that the farnesylation of these small GTPases by GGT-I may require an unidentified accessory factor, like Rab escort protein for GGT-II (3), in *E. histolytica*. Altogether, these results suggest that the substrate specificity of prenyltransferases varies widely among organisms. Further studies, including the cloning and enzymatic characterization of GGT-I of *E. histolytica* to determine if *Eh*Ras proteins are geranylgeranylated by the amebic GGT-I, are now underway.

Although we did not show a specific role for *Eh*Ras4, this protein shares all the conserved domains characteristic of Ras (42) except for incomplete DXAG and $D(X)_nT$ consensus sequences, and showed a close kinship to other *Eh*Ras proteins in the phylogenetic reconstruction (Fig. 6). We demonstrated that *Eh*Ras4 was capable of binding GTP (data not shown), verifying its identity as a small GTP-binding protein. *Eh*Ras1-4 lack a cysteine residue located 5–8 amino acids upstream of the C terminus to be palmitoylated in H- and N-Ras (45), which was shown to be essential for membrane association. In addition, *Eh*Ras4, in contrast to *Eh*Ras1-3, also lacks the so-called polybasic region (Fig. 5*A*), which was found in K-RasB and attributed to membrane association (46). The polybasic region was also implicated in interaction with a negatively charged patch on the surface of FTβ, which is located in close proximity to the region responsible for the binding to the Ras C terminus (38). Interestingly, *Eh*FTβ, which shows low affinity to *Eh*Ras1-3 with the polybasic region and high affinity toward *Eh*Ras4 without it, possesses a number of substitutions of negatively charged with either positively-charged or neutral amino acids particularly in helixes 3–5 (38) (*e.g.* D91S, E94M, E112R, D115G, E116Y, E131R, E166V, E167N, and D170Q, corresponding to rat FTβ). It is conceivable that these substitutions compensate for the repulsive force that interferes with proper binding, which would partially explain the observed Ras specificity of the amebic FT.

In addition to its unique (*i.e.* *Eh*Ras4-specific) acceptor specificity, the amebic FT revealed notable differences in sensitivity against compounds known to inhibit human FT by distinct mechanisms (Table I). Marked differences in sensitivity to FPP analogues were unexpected since all the aromatic amino acids (Trp^{102}, Tyr^{105}, Trp^{106}, Tyr^{154}, Tyr^{205}, Phe^{253}, Phe^{302}, Trp^{303}, Tyr^{361}, and Tyr^{365} of rat FTβ) that were shown to be located in the hydrophobic cleft at the center of the α-α barrel and implicated to be essential for the interaction with FPP within the FPP-binding pocket (41) were conserved. FPT inhibitors I, II, and α-hydroxyfarnesyl phosphonic acid share the common farnesyl (C15) portion (36), which interacts with these aromatic residues lined on this hydrophobic cleft (38). Therefore, the lack of sensitivity of *Eh*FT against these FPP analogues suggests that the binding specificity of these compounds does not depend on the structure of the FPP-binding pocket *per se*, but on the neighboring spacial and electrostatical environment. The fact that *Eh*FT is >10-fold more resistant to FPT inhibitor I and

α-hydroxyfarnesyl phosphonic acid than FPT inihibitor II whereas human FT is equally sensitive to these inhibitors agrees well with the notion that *Eh*FT has higher affinity to FPT inhibitor II. Considering the major structural differences between FPT inhibitors I and II: the presence of the *O*-ester linkage and the absence of the C-terminal residue in FPT inhibitor II, the observed differences in sensitivity may be partially explained by the substitutions of negative with neutral/positive amino acids found in the amebic FT described above. It is conceivable that *Eh*FT is not sensitive to the C*aa*M peptidomimetic FTI-276 (>1000-fold less than human FT) since *Eh*Ras3-CSVM was not a substrate of *Eh*FT. Finally, exploitation of critical differences in the affinity toward substrates and inhibitors between the mammalian and amebic FT should enable us to discover or design novel inhibitors selective for *Eh*FT, leading to the development of new chemotherapeutics against amebiasis.

Acknowledgments—We thank Naohiro Watanabe, Jikei, for valuable discussions and Yumiko Saito-Nakano and Fumie Tokumaru, NIID, for the *Eh*Rab5, *Eh*Rab7, and *Eh*Rap2 recombinant protein and helpful discussions. We also thank Vahab Ali, NIID, for the analysis of FT on gel filtration chromatography and Tomomi Okita, Jikei, for technical assistance. The data base search was conducted with a 7× *E. histolytica* genome data base available at the Institute for Genomic Research (TIGR) and Sanger Institute with financial support from NIAID, National Institutes of Health and The Wellcome Trust.

REFERENCES

1. Boguski, M. S., and McCormick, F. (1993) *Nature* **366,** 643–654
2. Takai, Y., Kaibuchi, K., Kikuchi, A., and Kawata, M. (1992) *Int. Rev. Cytol.* **133,** 187–230
3. Zang, F. L., and Casey, P. J. (1996) *Annu. Rev. Biochem.* **65,** 241–269
4. Moores, S. L., Schaber M. D., Mosser, S. D., Rands, E., O'Hara, M. B., Garsky, V. M., Marshall, M. S., Pompliano, D. L., and Gibbs, J. B. (1991) *J. Biol. Chem.* **266,** 14603–14610
5. James, G. L., Goldstein, J. L., and Brown, M. S. (1995) *J. Biol. Chem.* **270,** 6221–6226
6. Tabin, C. J., Bradley, S. M., Bargmann, C. I., Weinberg, R. A., Papageorge, A. G., Scolnick, E. M., Dhar, R., Lowy, D. R., and Chang, E. H. (1982) *Nature* **300,** 143–149
7. Reddy, E. P., Reynold, R. K., Santos, E., and Barbacid, M. (1982) *Nature* **300,** 149–152
8. Taparowsky, E., Suard, Y., Fasano, O., Shimizu, K., Goldfarb, M., and Wigler, M. (1982) *Nature* **30,** 762–765
9. Gibbs, J. B. (1991) *Cell* **65,** 1–4
10. Gelb, M. H., Van Voorhis W. C., Buckner, F. S., Yokoyama, K., Eastman, R., Carpenter, E. P., Panethymitaki, C., Brown, K. A., and Smith, D. F. (2003) *Mol. Biochem. Parasitol.* **126,** 155–163
11. World Health Organization (1997) *Bull. World Health Organ.* **75,** 291–292
12. Shen, P.-S., Lohia, A., and Samuelson, J. (1994) *Mol. Biochem. Parasitol.* **64,** 111–120
13. Shen, P.-S., Sanford, J. C., and Samuelson, J. (1996) *Exp. Parasitol.* **82,** 65–68
14. Lohia, A., and Samuelson, J. (1993) *Mol. Biochem. Parasitol.* **58,** 177–180
15. Lohia, A., and Samuelson, J. (1996) *Gene (Amst.)* **173,** 205–208
16. Ghosh, S. K., and Samuelson, J. (1997) *Infect. Immun.* **65,** 4243–42499
17. Guilen, N., and Sansonetti, P. (1997) *Arch. Med. Res.* **28,** 129–131
18. Guilen, N., Boquet, P., and Sansonetti P. (1998) *J. Cell Sci.* **111,** 1729–1739
19. Temesvari, L. A., Harris, E. N., Stanley, S. L., Jr., and Cardelli, J. A. (1999) *Mol. Biochem. Parasitol.* **103,** 225–241
20. Juarez, P., Sanchez-Lopez, R., Ramos, M. A., Stock, R. P., and Alagon, A. (2000) *Arch. Med. Res.* **31,** S157–159
21. Saito-Nakano, Y., Nakazawa, M., Shigeta, Y., Takeuchi, T., and Nozaki, T. (2001) *Mol. Biochem. Parasitol.* **116,** 219–222
22. Rodríguez, M., A., Garcia-Perez, R., M., Garcia-Rivera, G., Lopez-Reyes, I., Mendoza, L., Ortiz-Navarrete, V., and Orozco, E. (2000) *Mol. Biochem. Parasitol.* **108,** 199–206
23. Diamond, L. S., Mattern, C. F., and Bartgis, I. L. (1972) *J. Virol.* **9,** 326–341
24. Diamond, L. S., Harlow, D. R., and Cunnick, C. C. (1978) *Trans. R. Soc. Trop. Med. Hyg.* **72,** 431–432
25. Nozaki, T., Asai, T., Kobayashi, S., Ikegami, F., Noji, M., Saito, K., and Takeuchi, T. (1998) *Mol. Biochem. Parasitol.* **97,** 33–44
26. Tompson, J. D., Higgins, D. G., and Gibson, T. J. (1994) *Nucleic Acids Res.* **22,** 4673–4680
27. Saitou, N., and Nei, M. (1987) *Mol. Biol. Evol.* **4,** 406–425
28. Page, R. D. (1996) *Comput. Appl. Biosci.* **12,** 357–358
29. Felsenstein, J. (1985) *Evolution* **39,** 783–791
30. Higuchi, R. (1990) in *PCR Protocols: A Guide to Methods and Applications* (Innnis, M. A., Gelfand, D. H., Shinsky, J. J., and White, T. J., eds) pp. 177–183, Academic Press, New York
31. Omer, C. A., Diehl, R. E., and Kral, A. M. (1995) *Methods Enzymol.* **250,** 3–21
32. Nepomuceno-Silva, J., L., Yokoyama, K., de Mello, L. D. B., Mendonça, S. M., Paixão, J. C., Baron, R., Faye, J.-C., Buckner, F. S., Van Voorhis, W. C., Gelb, M. H., and Lopes, U. G. (2001) *J. Biol. Chem.* **276,** 29711–29718
33. Bradford, M. M. (1976) *Anal. Biochem.* **72,** 248–254
34. Sambrook, J., Fritsch, E. F., and Maniatis, T. (1989) *Molecular Cloning: A Laboratory Manual*, pp. 18.47–18.57, Cold Spring Harbor Laboratory Press, Cold Spring Harbor, NY
35. Pompliano, D. L., Rands, E., Schaber, M. D., Mosser, S. D., Anthony, N. J., and Gibbs, J. B. (1992) *Biochemistry* **31,** 3800–3807
36. Manne, V., Yamazaki, S., and Kung, H.-F. (1984) *Proc. Natl. Acad. Sci. U. S. A.* **81,** 6953–6957
37. Boguski, M. S., Murray, A. W., and Powers, S. (1992) *New Biologist* **4,** 408–411
38. Park, H. W., Boduluri, S. R., Moomaw, J. F., Casey P. J., and Beese, L. S. (1997) *Science* **21,** 1800–1804
39. Kral, A. M., Diehl, R. E., deSolms, S. J., Williams, T. M., Kohl, N. E., and Omer, C. A. (1997) *J. Biol. Chem.* **272,** 27319–27323
40. Dunten, P., Kammlott, U., Crowther, R., Weber, D., Palermo, R., and Birktoft, J. (1998) *Biochemistry* **40,** 7907–7912
41. Micali, E., Chehade, K. A., Isaacs, R. J., Andres, D. A., and Spielmann, H. P. (2001) *Biochemistry* **40,** 12254–12265
42. Bourne, H. R., Sanders, D. A., and McCormick, F. (1991) *Nature* **349,** 117–127
43. Yokoyama, K., Lin, Y., Stuart K. D., and Gelb, M. H. (1997) *Mol. Biochem. Parasitol.* **87,** 61–69
44. Armstrong, S. A., Hannah, V. C., Goldstein, J. L., and Brown, M. S. (1995) *J. Biol. Chem.* **270,** 7864–7868
45. Hancock, J. F., Anthony, I., Magee, I., Childs, J. E., and Marshall, C. J. (1989) *Cell* **57,** 1167–1177
46. Hancock, J. F., Paterson, H., and Marshall, C. J. (1990) *Cell* **63,** 133–139
47. Manne, V., Ricca, C. S., Brown, J. G., Tuomari, A. V., Yang, N., Patel, D., Schmidt, R., Lynch, M. J., Ciosek, C. P., Jr., Carboni J. M., Robinson, S., Gordonm E. M., Barbacid, M., Seizinger, B. R., and Biller, S. A. (1995) *Drug Development Res.* **34,** 121–137
48. Van der Pyl D., Inokoshi, J., Shiomi, K., Yang, H., Takeshima, H., and Omura, S. (1992) *J. Antibiot. (Tokyo)* **45,** 1802–1805
49. Gibbs, J. B., Pompliano, D. L., Mosser, S. D., Rands, E., Lingham, R. B., Singh, S. B., Scolnick, E. M., Kohl, N. E., and Oliff, A. (1993) *J. Biol. Chem.* **268,** 7617–7620
50. Lernar, E. C., Qian, Y., Blaskovich, M. A., Fossum, R. D., Vogt, A., Sun, J., Cox, A. D., Der C. J., Hamilton, A. D., and Sebti, S. M. (1995) *J. Biol. Chem.* **270,** 26802–26806

Parasitol Res (2004) 93: 68–71
DOI 10.1007/s00436-004-1106-8

ORIGINAL PAPER

Asao Makioka · Masahiro Kumagai · Seiki Kobayashi
Tsutomu Takeuchi

Different effects of cytochalasins on the growth and differentiation of *Entamoeba invadens*

Received: 9 February 2004 / Accepted: 19 February 2004 / Published online: 21 April 2004

Abstract The effect of five different cytochalasins on the growth, encystation and excystation of *Entamoeba invadens* was examined. At 10 μM, cytochalasins B, D, E and dihydrocytochalasin B markedly inhibited growth. Encystation was inhibited by cytochalasin D at 1 μM but not by other cytochalasins at the same concentration, whereas it was inhibited by 10 μM of cytochalasins B, E and dihydrocytochalasin B as well as cytochalasin D. Excystation, which was assessed by counting the number of metacystic amoebae after inducing excystation, was markedly enhanced by cytochalasin D as previously demonstrated, whereas the enhancing effect of cytochalasins A, B and dihydrocytochalasin B was weak. In contrast, cytochalasin E at 10 μM inhibited excystation and metacystic development. These results indicate that there is a difference in the effect of different cytochalasins on the growth and differentiation of *E. invadens*, depending on differences in their chemical structure.

Introduction

Cytochalasins are cell-permeable fungal toxins. The primary effect of cytochalasins is to inhibit actin polymerization, but these compounds also affect functions not yet known to be related to the actin cytoskeleton, such as glucose transport and mitochondrial respiration (Lin and Spudich 1974; Brenner and Korn 1980; Flanagan and Lin 1980; Manavanthu et al. 1980). Unlike cytochalasins A and B, cytochalasins D and E do not inhibit glucose transport. Structurally, cytochalasins are a family of compounds characterized by a central perisohydroindole core ring and a large attached macrocyclic ring which varies in size and composition.

Studies on the differentiation of *Entamoeba histolytica*, including encystation and excystation, are difficult because there is no axenic encystation medium available for this parasite (López-Romero and Villagómez-Castro 1993). The in vitro axenic encystation and excystation of *E. invadens*, a reptilian parasite, are useful models for the encystation and excystation of *E. histolytica* because these processes in the human parasite are similar to those of *E. invadens* (Dobell 1928; Cleveland and Sanders 1930; Geiman and Ratcliffe 1936; López-Romero and Villagómez-Castro 1993). Transfer of *E. invadens* trophozoites from a growth medium to an encystation medium induces encystation (Sanchez et al. 1994), and the transfer of cysts from an encystation medium to a growth medium induces excystation (McConnachie 1955; Rengpien and Bailey 1975; Garcia-Zapien et al. 1995; Makioka et al. 2001). Using an in vitro system for the encystation and excystation of *E. invadens*, we previously demonstrated that cytochalasin D inhibits the growth and encystation of *E. invadens*, with encystation being more sensitive to the drug than growth (Makioka et al. 2000). Like cytochalasins, latrunculins inhibit actin polymerization, whereas jasplakinolide promotes actin polymerization and stabilizes polymerized actin (Spector et al. 1983; Bubb et al. 1994). We demonstrated that cytochalasin D unexpectedly enhances the excystation and metacystic development of *E. invadens*, although latrunculin A and jasplakinolide inhibit these processes (Makioka et al. 2001). From these results, we considered it of interest to determine whether other cytochalasins exhibit similar effects to cytochalasin D on the growth and differentiation of *E. invadens*.

A. Makioka (✉) · M. Kumagai
Department of Tropical Medicine,
Jikei University School of Medicine,
3-25-8 Nishi-shinbashi, Minato-ku, Tokyo 105-8461, Japan
E-mail: makioka@jikei.ac.jp
Tel.: +81-3-34331111
Fax: +81-3-34314459

S. Kobayashi · T. Takeuchi
Department of Tropical Medicine and Parasitology,
Keio University School of Medicine, 35 Shinanomachi,
Shinjuku-ku, Tokyo 160-8582, Japan

Materials and methods

Trophozoites of *E. invadens* strain IP-1 were cultured in axenic growth medium BI-S-33 (Diamond et al. 1978) at 26°C. For experiments on the effect of cytochalasins on growth, trophozoites (10^4 cells/ml) were cultivated in the growth medium including 1 μM or 10 μM of cytochalasins A, B, D, E, or dihydrocytochalasin B for 7 days and then counted. For experiments on encystation, trophozoites (5×10^5 cells/ml) were transferred to the encystation medium 47% LG (LG is BI without glucose; Sanchez et al. 1994) containing 1 μM or 10 μM of the cytochalasins above. After 3 days of incubation, trophozoites and cysts were counted, and their viability determined by trypan blue exclusion and the percentage encystation was determined. For experiments on excystation, the cells were harvested after 3 days' incubation of trophozoites in the encystation medium and treated with 0.05% sarkosyl (Sigma Chemical, St. Louis, Mo.) to destroy the trophozoites (Sanchez et al. 1994). The remaining cysts were washed with phosphate-buffered saline, counted and suspended in a growth medium. Viability of the cysts was determined by trypan blue exclusion. Duplicate cultures of 5×10^5 cysts/ml included 1 μM or 10 μM of cytochalasins. These were incubated for 3 days. Viable metacystic amoebae and cysts were clearly distinguished, being pale yellow and light blue, respectively. The former was also identified by positive motility. The five cytochalasins used, A, B, D, E and dihydrocytochalasin B, were purchased from Calbiochem (San Diego, Calif.) and were initially dissolved in dimethyl sulfoxide (DMSO). The control cultures received the same volume of DMSO.

Results

Effect of cytochalasins on growth

The effect of the five cytochalasins on the growth of *E. invadens* is shown in Fig. 1. All cytochalasins used at 1 μM had no effect on the growth of *E. invadens*. With 10 μM of cytochalasins B, D, E and dihydrocytochalasin B, markedly inhibited growth was observed, whereas cytochalasin A at 10 μM had no effect.

Effect of cytochalasins on encystation

The results of encystation are shown in Fig. 2. Control cultures produced about an 80% cyst yield at 3 days after the induction of encystation (data not shown). At 1 μM of cytochalasin D, 70% inhibition of the control encystation was found, whereas other cytochalasins at 1 μM had no inhibitory effect. At 10 μM of cytochalasin B, dihydrocytochalasin B, cytochalasin D and cytochalasin E 85%, 30%, 82%, and 100% inhibition occurred,

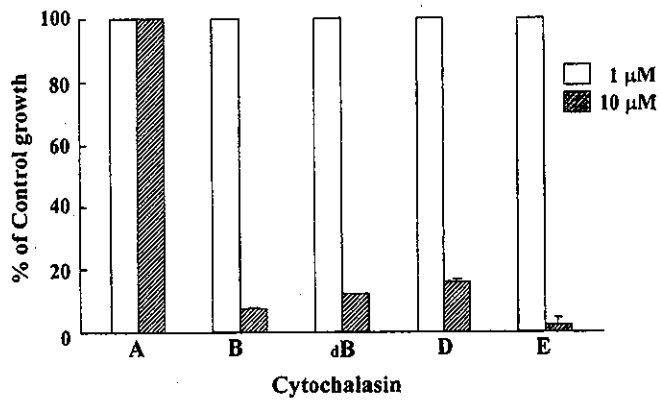

Fig. 1 Effect of cytochalasins on the growth of *Entamoeba invadens*. Trophozoites were cultured for 7 days in the presence of 1 μM or 10 μM cytochalasins A, B, D, E and dihydrocytochalasin B (*dB*). Control growth was measured in the absence of the drug and was expressed as 100%. The percentages ± SE of the control growth for duplicate cultures are plotted

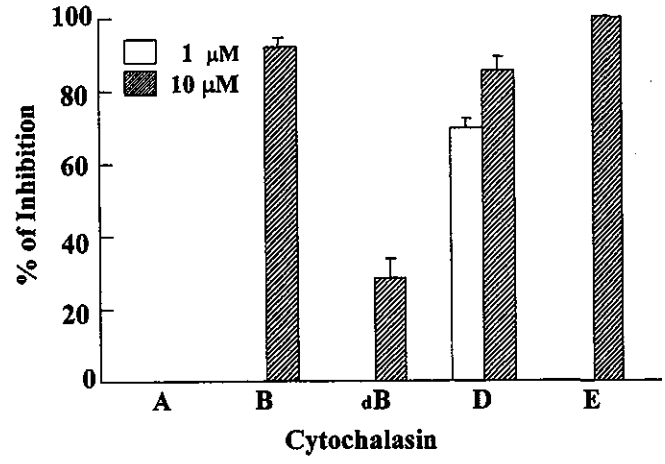

Fig. 2 Effect of cytochalasins on the encystation of *E. invadens*. Trophozoites were transferred to an encystation medium containing 1 μM or 10 μM cytochalasins A, B, D, E and dihydrocytochalasin B (*dB*). The cysts and trophozoites were counted to determine the percentages of cysts 3 days later. Control encystation was 80%. The percentages ± SE of inhibition against the control encystation for duplicate cultures are plotted

respectively, of the control encystation, whereas cytochalasin A at 10 μM had no inhibitory effect.

Effect of cytochalasins on excystation and metacystic development

The effect of cytochalasins on the number of metacystic amoebae is shown in Fig. 3. Cytochalasin D at 1 μM induced a marked increase in the number of metacystic amoebae from 5 to 48 h of incubation compared to the controls, which is consistent with our previous results (Makioka et al. 2001). In contrast, other cytochalasins at 1 μM had little effect on the number of metacystic amoebae compared to the controls except for the increase in number due to cytochalasin E at 48 and 72 h.